Published in final edited form as:

Nat Med. 2021 December ; 27(12): 2154–2164. doi:10.1038/s41591-021-01550-z.

Long-term ecological assessment of intracranial electrophysiology synchronized to behavioral markers in Obsessive-Compulsive Disorder

Nicole R. Provenza[1,2], **Sameer A. Sheth**[3], **Evan M. Dastin-van Rijn**[1], **Raissa K. Mathura**[3], **Yaohan Ding**[4], **Gregory S. Vogt**[5], **Michelle Avendano-Ortega**[5], **Nithya Ramakrishnan**[5], **Noam Peled**[6,7], **Luiz Fernando Fracassi Gelin**[8], **David Xing**[1], **Laszlo A. Jeni**[9], **Itir Onal Ertugrul**[10], **Adriel Barrios-Anderson**[11], **Evan Matteson**[1], **Andrew D. Wiese**[5,12], **Junqian Xu**[5,13], **Ashwin Viswanathan**[3], **Matthew T. Harrison**[14], **Kelly R. Bijanki**[3,5], **Eric A. Storch**[5], **Jeffrey F. Cohn**[15], **Wayne K. Goodman**[5,†], **David A. Borton**[1,16,17,†,*]

[1]Brown University School of Engineering, Providence, RI, United States.

[2]Charles Stark Draper Laboratory, Cambridge, MA, United States.

[3]Department of Neurosurgery, Baylor College of Medicine, Houston, TX, United States.

[4]Intelligent Systems Program, University of Pittsburgh, Pittsburgh, PA, United States.

[5]Menninger Department of Psychiatry and Behavioral Sciences, Baylor College of Medicine, Houston, TX, United States.

[6]MGH/HST Martinos Center for Biomedical Imaging, Charlestown, MA, United States.

[7]Harvard Medical School, Cambridge, MA, United States.

[8]Center for Computation and Visualization, Brown University, Providence, RI, United States.

[*]Corresponding author: David Borton; 401-863-2963 (phone); 401-863-9028 (fax); david_borton@brown.edu; 184 Hope Street Providence, RI USA.

[†]Co-senior authors

Author contributions statement: WKG, JFC, SAS, and DAB conceived of the study. NRP conceptualized data analysis procedures, performed data analysis, interpreted data, and prepared figures and results with support from EMDVR, MTH, RKM, NP, YD, ABA, SAS, and DAB. EMDVR carried out packet loss correction and artifact removal procedures with support from NRP and MTH. JX optimized the MRI protocol. RKM, NP, KB, and NRP performed MRI analysis, and NP developed the MMVT software. LAJ and IOE developed AFAR analysis methodology. YD and LAJ performed AFAR analysis, and NRP, LAJ, and YD created the supplementary videos. GSV, MAO, NR, and NRP performed data collection in the clinic. ERM supported data collection. NRP, GSV, and MAO guided participant data collection at home. ADW provided clinical ERP sessions, and ADW and NRP collected data during ERP, supervised by EAS. ABA documented SUDs ratings using ERP videos. LFFG and DX created new software to enable the collection of intracranial electrophysiology at home. NRP and SAS wrote the first draft of the manuscript and all authors contributed to the writing and revision of the manuscript. WKG, SAS, AV, and EAS performed the clinical care aspects of the study. SAS and AV performed the study surgical procedures. WKG, SAS, JFC, EAS, and DAB oversaw the collection of data, analysis, and manuscript completion.

Competing interests statement: DAB and WKG received device donations from Medtronic as part of the NIH BRAIN public-private-partnership program (PPP). WKG received honoraria from Biohaven Pharmaceuticals. SAS has consulting agreements with Boston Scientific, Neuropace, Koh Young, Zimmer Biomet, and Abbott. NP is a co-founder and stocks holder at FIND Surgical Sciences Inc. The remaining authors declare no competing interests.

Data Availability: The complete datasets generated (excluding video/audio) and analyzed during the current study will be made publicly available at study completion and will be deposited in the NIH Data Archive for the Brain Initiative®. The minimum dataset required to reproduce all results of the manuscript (excluding video and audio) is publicly available through the associated Open Science Framework project, DOI: 10.17605/OSF.IO/YQA2K.

Code Availability: Custom code used to produce the results in this manuscript is available at https://github.com/neuromotion/ecological-ephys-behav-ocd.

[9]Robotics Institute, Carnegie Mellon University, Pittsburgh, PA, United States.

[10]Department of Cognitive Science and Artificial Intelligence, Tilburg University, Tilburg, The Netherlands.

[11]The Warren Alpert Medical School of Brown University, Providence, RI, United States.

[12]Department of Psychology, University of Missouri - Kansas City, Kansas City, MO, United States.

[13]Department of Radiology, Baylor College of Medicine, Houston, TX, United States.

[14]Division of Applied Mathematics, Brown University, Providence, RI, United States

[15]Department of Psychology, University of Pittsburgh, Pittsburgh, PA, United States.

[16]Carney Institute for Brain Science, Brown University, Providence, RI, United States.

[17]Center for Neurorestoration and Neurotechnology, Rehabilitation R&D Service, Department of Veterans Affairs, Providence, RI, United States.

Abstract

Detection of neural signatures related to pathological behavioral states could enable adaptive deep brain stimulation (aDBS), a potential strategy for improving efficacy of DBS for neurological and psychiatric disorders. This approach requires identifying neural biomarkers of relevant behavioral states, a task best performed in ecologically valid environments. Here, in human participants with obsessive-compulsive disorder (OCD) implanted with recording-capable DBS devices, we synchronized chronic ventral striatum local field potentials (LFP) with relevant, disease-specific behaviors. We captured over 1,000 hours of LFP in the clinic and at home during unstructured activity, as well as during DBS and exposure therapy. The wide range of symptom severity over which the data were captured allowed us to identify candidate neural biomarkers of OCD symptom intensity. This work demonstrates the feasibility and utility of capturing chronic intracranial electrophysiology during daily symptom fluctuations to enable neural biomarker identification, a prerequisite for future development of aDBS for OCD and other psychiatric disorders.

Obsessive-compulsive disorder (OCD) has a lifetime prevalence of 2–3% and is a leading cause of disability worldwide [1]. Pharmacological and cognitive-behavioral therapy are the mainstays of treatment but fail to provide sustained benefit in 25–40% of individuals [1]. Approximately 10% of individuals fail to achieve benefit from any intervention [2]. For severe, treatment-refractory cases of OCD, neurosurgical procedures have been used with varying degrees of success for half a century [1]. Modern neurosurgical approaches include both stereotactic lesion procedures and deep brain stimulation (DBS), with roughly similar response rates [1]. Over half of patients with treatment-resistant OCD are responders to DBS targeted to the ventral capsule/ventral striatum (VC/VS) region [3]. Beyond marked improvement in OC symptoms, VC/VS DBS has been found to improve anxiety, depression, mood, and quality of life even in patients who are non-responders to DBS treatment [4,5]. To date, the number of patients who have received DBS for OCD worldwide is in the hundreds

[6]. Many more individuals may qualify for DBS but do not receive or pursue this treatment course due to various barriers (e.g., awareness, access, cost) or treatment preferences.

One of the main advantages of DBS over other neurosurgical approaches (e.g., stereotactic lesion procedures) is its adjustability. Stimulation parameters can be varied and optimized to maximize beneficial effects and minimize adverse effects. This programmability is an important reason why DBS is more common than lesion procedures in the surgical treatment of movement disorders such as Parkinson's disease and essential tremor [7]. However, adjusting DBS parameters for OCD management differs significantly from that for movement disorders. Whereas stimulation effects (both beneficial and adverse) typically occur over seconds to minutes in movement disorders, the delay is much longer in psychiatric disorders. Reductions in OCD symptoms usually manifest weeks to months after initiation of DBS stimulation [4], producing a mismatch in time constants between an adjustment and its effect. Further complicating management is the natural temporal variation of symptom severity within individuals [8]. These factors together impose great barriers to the clinician's attempt to align stimulation parameter adjustments with the moving target of symptom fluctuations.

An emerging strategy for surmounting these challenges is the development of adaptive, responsive, closed-loop DBS [9–11]. Current DBS therapy often operates in an open loop, wherein parameter adjustments are made *ad hoc* during periodic clinic visits weeks or months apart. Continuous stimulation at fixed parameters between clinical visits may inadequately address the temporal dynamics of neurological or psychiatric illnesses, in which symptoms vary over minutes to days. Additionally, stimulation can cause undesirable side effects if applied when not needed [3]. A responsive, closed-loop, adaptive DBS (aDBS) system may improve efficacy by titrating stimulation parameters in response to real-time neural signatures (i.e., biomarkers) related to symptoms and side effects.

The last few years have witnessed a rapid expansion in the application of aDBS strategies and technology for use in movement disorders [12–15]. Successful demonstrations of aDBS, notably in Parkinson's Disease, have emphasized the need for reliable, symptom specific behavioral readouts that map to electrophysiological biomarkers [16]. For example, beta-band power in the subthalamic nucleus (STN) is a well-recognized candidate biomarker for certain symptoms in Parkinson's disease [17]. Unlike in movement disorders, however, there is currently no objective behavioral readout (e.g., diminished tremor in Parkinson's Disease) in psychiatric disorders that clinicians can gauge in real time to optimize DBS parameters. Instead, in psychiatric disorders, clinicians rely on standardized subjective symptom scales in order to guide therapy delivery such as DBS parameter adjustments [18].

These two factors – the temporal mismatch between symptom evolution and typical DBS adjustment schedule, and the lack of an objective biomarker of psychiatric symptom severity – highlight the monumental challenges facing psychiatric neurosurgery. At the same time, they also underscore the great opportunity for aDBS [19]. Our work seeks to address these challenges by recording neural activity during natural, day-to-day OCD symptom fluctuations to begin understanding these critical neural-behavioral relationships.

Recently available devices have provided the technology necessary for both streaming brain electrophysiology data and performing closed-loop control of stimulation parameters [20,21]. Wireless streaming of neural data outside the clinic is key to robust biomarker discovery, as it enables the collection of neural data under ecological conditions and over extended periods of time, capturing the dynamics of symptom state and neural correlates of behavior. Others have demonstrated feasibility and utility of such platforms for recording at home from participants with epilepsy and Parkinson's Disease [22–24].

Here, we present the first longitudinal collection of electrophysiology, behavior, and clinical evaluations from five participants with severe, refractory OCD treated with DBS as part of an ongoing clinical trial towards developing aDBS for OCD (NCT04281134, NCT03457675). For the first time in patients with a psychiatric disorder, we demonstrate the utility of not only in-clinic, but also at-home collection of time-synchronized, multi-modal brain and behavioral data, which vastly increase both the quantity and ecological validity of the recorded data. We used computer vision machine learning techniques on face video recordings to assess moment to moment changes in emotional state, time-locked with intracranial and extracranial neural recordings. We have captured over 1000 hours of intracranial recordings during behavioral tasks and daily activities at home labelled with ecological momentary assessment of symptom state. Additionally, we conducted intracranial VC/VS recordings during provocations of symptoms with concomitant administration of two treatment modalities: DBS and Exposure and Response Prevention (ERP) teletherapy. Lastly, based on a series of pilot recordings collected during natural OCD exposures and ERP teletherapy, we demonstrate the ability to measure VC/VS spectral power during natural OCD symptom provocations at home. Continued opportunities for long-term, naturalistic intracranial electrophysiological recordings will propel biomarker discovery for OCD and other psychiatric disorders.

Results

Study design

Five participants (P1, P2, P3, P4, and P5) with long-standing refractory OCD underwent surgery for bilateral placement of DBS leads capable of applying stimulation and bipolar sensing of neural activity. Longitudinal intracranial electrophysiology was collected in the clinic and at home in three study participants (P3, P4, and P5). Electrophysiological recordings were time-locked to behavior and DBS parameter changes in the clinic, and momentary self-report of OCD symptoms, ERP therapy, and behavioral tasks at home (Figure 1).

Information on participant demographics, stimulation contact, bipolar sensing contact pair, stimulation parameters, and responder status, defined by 35% reduction in Yale-Brown Obsessive Compulsive Scale II (Y-BOCS II) score [25], is included in Extended Data Table 1. All five participants were responders to DBS therapy (Extended Data Table 1).

DBS electrodes target the VC/VS and BNST

Leads were placed in either the ventral striatum (VS) or bed nucleus of the stria terminalis (BNST) and suprajacent white matter based on intraoperative findings during awake testing. Due to individual specificity, therapeutic response was evaluated on both sides of the anterior commissure (AC) in order to determine the optimal stimulation target within the broader VC/VS region. In participants P1 and P2, stimulation targets were the left and right BNST (Extended Data Fig. 1). In participant P3, stimulation targets were the left and right VS (Extended Data Fig. 1). In participant P4, stimulation targets were the left VS and right BNST (Fig. 2 A-E), and in participant P5, the left and right BNST (Extended Data Fig. 1).

Participants P1 and P2 were implanted with the Activa PC+S® system, and participants P3, P4, and P5 were implanted with the Summit RC+S® system. The Medtronic Summit RC+S® rechargeability and wireless data transmission enables streaming of time-domain intracranial electrophysiology both in the clinic and at home not possible with the Activa PC+S® system, or any other therapeutic DBS platform. In addition, the Medtronic Summit RC+S® system offers improved artifact rejection and sensing performance compared to the Activa PC+S® system [20]. Therefore, herein we focus on data gathered from the three participants implanted with the Summit RC+S®.

Longitudinal recordings show stability over time

To gauge the quality of the longitudinal recordings over time, impedance of sensing and stimulation electrodes for P3, P4, and P5 was measured over the course of the study (Extended Data Fig. 2). Variation in impedance between the sensing contacts and implanted neural stimulator (INS) hermetic enclosure (i.e., case) ranged from 705 Ohms to 1303 Ohms for P3 over 101 days, 933 Ohms to 1910 Ohms for P4 over 405 days, and 703 Ohms to 1468 Ohms for P5 over 181 days (all measured at 100 Hz), reflecting long-term stability in the device-tissue interface.

Increase in positive affect captured during DBS programming

During clinical DBS programming sessions, intracranial electrophysiological signals were synchronized to behavioral, physiological, and electrophysiological measures in order to develop biomarkers for closed-loop control of stimulation. We used video of the participant's face (Fig. 3A) to estimate positive affect (Fig. 3B) and head velocity (Fig. 3C) as objective measures of the anxiolytic and anxiogenic responses to changes in DBS parameters (see Methods). Positive affect was estimated using Automatic Facial Affect Recognition (AFAR), which provides an objective, well-validated approach to quantify subtle changes in affective responses (i.e., mirth, smiles, and brow furrows) intraoperatively and thereafter [26]. Additionally, we recorded external electrophysiological signals, including blood volume pulse (BVP), electrocardiogram (ECG) (Fig. 3D), and 64-channel electroencephalography (EEG) (Fig. 3E) and synchronized these signals to changes in DBS parameters (e.g., DBS amplitude) (Fig. 3F), VS and/or BNST LFP recordings (Fig. 3G), and Summit RC+S® acceleration (Fig. 3H). As a demonstrative example, we observed an increase in P5's positive affect in response to an increase in stimulation amplitude, highlighted by a captured smile corresponding to the peak in positive affect estimation during a period of DBS programming where amplitude was incrementally increased from

zero to 4.5 mA in steps of 0.5 mA. During and following an increase in DBS amplitude, participant P5 also described positive feelings, including a physical sensation that she was no longer “internally trembling” (Supp. Video 1). Clinical experience and limited empirical data suggest that this subjective, positive response to increase in DBS amplitude is a typical response that may be predictive of treatment outcome [27].

Intracranial LFP during natural symptom variation at home

We then sought to collect intracranial electrophysiology in more ecologically valid conditions by using the Summit RC+S® to wirelessly stream intracranial electrophysiology during routine activities in the participants’ homes. At home, participants used a custom tablet application (frontend: https://github.com/openmind-consortium/App-OCD-PatientFrontend, backend: https://github.com/openmind-consortium/App-OCD-PatientBackend) to initiate intracranial VC/VS and/or BNST recordings and perform psychophysiological tasks (https://github.com/brown-ccv/honeycomb) [28]. Participants reported their OCD symptom intensity and sleep start/stop times using the StriveStudy OCD mobile application (Rune Labs; iPhone XR). Self-report measures were time-synchronized with electrophysiology recordings via network time protocol (see Methods). Self-reported intensity of OCD symptoms and Y-BOCS II were collected after DBS was turned on for participants P3, P4, and P5 (Fig. 4A). Y-BOCS II was administered during clinical visits, while self-reported symptom intensity was captured on a daily basis, or more frequently, by each participant through the StriveStudy OCD application. Interestingly, self-report values for P4 show that even after a significant reduction in Y-BOCS II score at week 27, a high day-to-day variability in symptom intensity (range: 0–8, std: 0.43–2.81) remained between clinical visits. Such variation in self-reports may have many sources, but motivates the need for an adaptive control system to titrate neuromodulation therapy to symptom dynamics. Participants P3 and P5 exhibited less variability in symptom intensity: 6–8 and 4–9, respectively (P3 std: 0–0.5; P5 std: 0–1.34).

While untreated OCD has a stable course [29], symptom intensity and severity is recognized to fluctuate within shorter time intervals (e.g., hours, days) [30]. Therefore, it was critical to develop a technology platform capable of collecting large datasets over long time periods. In total to-date, P3, P4, and P5 have collected 52, 813, and 207 hours of Summit RC+S® intracranial electrophysiology and accelerometry data at home, respectively (Fig. 4B), totally over 1000 hours. Each intracranial neural recording was matched to self-reported OCD symptom intensity ratings, behavioral tasks, and ERP teletherapy sessions. Behavioral tasks relevant to functional domains implicated in OCD were self-administered once per week at home during participant-controlled neural recording sessions (see Methods). We synchronized task behavior with neural recordings and calculated the number of hours of neural data collected during behavioral tasks for each participant (P3: 15 hours, P4: 37 hours, P5: 8 hours). Participant P4 did a multi-day “sprint recording” during which over 24 hours of data were collected, including Apple Watch heart rate and acceleration, RC+S® acceleration and LFP, and self-reported intensity of OCD symptoms (Fig. 4C, D).

Intracranial LFP during planned and natural exposures

Capturing intracranial electrophysiology during ERP teletherapy sessions is particularly relevant toward the goal of identifying a neural biomarker of OCD-related distress. The capability to record intracranial electrophysiology that is time-locked to naturalistic exposures to OCD triggers at home is a critical technological advancement that may enable discovery of ecologically valid biomarkers in psychiatry. During ERP teletherapy sessions, we recorded video of the participant and clinician during OCD trigger exposures (Fig. 5B). Throughout the ERP sessions, participants were asked to rate their Subjective Units of Distress (SUDs) in response to each exposure at various time intervals (Fig. 5C). SUDs ratings across all ERP sessions ranged from 4 to −6 for P3, and 3 to −10 for P4, and 1 to 8 for P5 (Extended Data Fig. 3). We synchronized ERP teletherapy video and SUDs ratings to LFP, and Summit RC+S® and Apple Watch acceleration and heart rate for participants P3 (Extended Data Fig. 4), P4 (Fig. 5D, Supp. Video 2), and P5 (Extended Data Fig. 5).

To demonstrate the utility of at-home data collection toward biomarker identification, we sought to gain insight on how spectral power changes with OCD symptoms. We analyzed neural data collected from P4 during a three-day continuous recording session. A total of 41 OCD symptom intensity ratings ranging from zero to eight were reported during neural recordings over the three-day span ($\mu = 4.49 \pm 2.57$) (Fig. 6A). We chose this particular recording for analysis and demonstration due to the occurrence of natural exposures that led to relatively high variability and range in self-reported OCD symptom intensity. Average normalized spectral band power in predefined frequency bands of interest (Delta: 0–4 Hz, Theta: 4–8 Hz, Alpha: 8–15 Hz, Beta: 15–30 Hz, and Gamma 30–55 Hz) was computed for LFP data collected one minute before and after each self-report (see Methods). Delta-band power in particular showed a strong negative correlation with OCD symptom intensity in both the left (Fig. 6B; $R = -0.593$) and right (Fig 6C; ($R = -0.557$) VC/VS. While the data suggest that the correlation between delta-band power and symptom intensity may be statistically significant, more investigation will be required to determine the consistency of this relationship across individuals. All other frequency bands of interest (Theta: 4–8 Hz, Alpha: 8–15 Hz, Beta: 15–30 Hz, and Gamma 30–55 Hz) exhibit relatively weaker correlations with OCD symptom intensity (absolute $R < 0.343$).

We repeated the same spectral analysis for one ERP session during concurrent intracranial neural recordings for participants P3, P4, and P5, and found variable correlations between spectral power in between frequency bands and SUDs ratings (Extended Data Fig. 6–8). These analyses reveal the utility of chronic intracranial LFP for identifying relationships between neural activity and behavior (in this case, psychiatric symptoms). In one participant (P4), the relationship we observed between delta-band spectral power and self-reported symptoms was preserved across natural exposures (Fig. 6B) and planned exposures during ERP teletherapy (Extended Data Fig. 7). Future work will determine the degree of consistency of these brain-behavior relationships across patients and their potential as a biomarker for aDBS applications.

Discussion

Wireless streaming of intracranial electrophysiology data in both the clinic and in naturalistic environments provides a rich data source for biomarker discovery. An electrophysiological biomarker of symptom state would enable aDBS for OCD and other psychiatric disorders, which may provide a better approach for treating fluctuations in symptom intensity [11]. Here, we acquired electrophysiological data with behavioral readouts over both short and long timescales. In the clinic, we examined changes in affect (AFAR) during DBS parameter changes over short timescales (seconds to minutes). At home during participant-controlled recordings, we captured behavioral changes (self-reported OCD symptoms) over longer timescales (days to weeks to months) in natural settings, collected continuous data during natural and planned exposures, and developed methods to synchronize behavioral metrics to intracranial electrophysiology. Further, we demonstrated the utility of at-home data collection for biomarker identification by observing correlations between spectral power and self-reported OCD symptom intensity.

Only with recent advances in device technology is it now possible to collect intracranial electrophysiology time synchronized with rich behavioral markers in ecologically valid environments from patients with neurological or psychiatric disorders. For example, Gilron et al. have described a platform for simultaneous intracranial electrophysiology and wearable accelerometer sensors in natural settings with Parkinson's disease patients [24]. As an example using another recording-capable device, Topalovic et al. have described a platform for simultaneous EEG, wearable sensors, VR, and intracranial electrophysiology, all contained in a small backpack. Their work demonstrates a major advance in collecting both a neurally and behaviorally rich dataset in freely moving humans [23]. Here, we demonstrated the first application of recent technological advances to record intracranial electrophysiology time-locked with behavioral events in patients with a psychiatric disorder in natural settings and at chronic timescales.

Conducting ecological recordings with a psychiatric population poses several key challenges that are important to address in future work. First, compliance of study participants is variable, and self-report psychological data is often inaccurate [31]. Intracranial electrophysiology collected over a wide, dynamic range of symptom severity is needed to build a classifier, and such a range may not always be available. We have observed that participants are more likely to comply with daily recordings when they are feeling well, and more likely to avoid engaging in recordings when OCD symptoms are exacerbated. Such reporting bias inherently limits the ecological nature of these recordings. Until we have the ability to trigger home recordings without engagement from the participant, the timing of naturalistic recordings will always be subject to the participant's motivation, anxiety, and mood. Additionally, a lack of overlap in OCD subtypes and timescales of symptom fluctuation among our small cohort of participants will likely require personalization of biomarkers and adaptive stimulation paradigms.

In future experiments, we expect to need to implement more extensive mood and symptom logging at home, in addition to tracking more objective measures of patient state such as activity level (e.g., number of steps, distance travelled from home) and engagement in social

activities (e.g., smartphone use). The utility of self-report assessments is limited as they rely on patient insight into their own psychological state, which is variable [31]. Additionally, we have observed that some participants may become superstitious about acknowledging that OCD symptoms have subsided and tend to report a stagnant trend in symptom intensity even after experiencing clinical benefit. More quantitative and objective measures have proven to be useful for tracking Parkinson's disease severity at home and could prove to have equal utility for tracking severity of psychiatric symptoms [32].

Additional studies should examine the behavioral task data we collected both in the clinic and at home to assess function in cognitive control, impulsivity, and evidence accumulation. Candidate biomarkers may not pertain to symptoms but instead to cognitive domains where function may be impaired. Administration of behavioral tasks allows for orthogonalization onto neurobiological axes (i.e., the Research Domain Criteria) that could provide useful information for relating mental processes to electrophysiology [33,34]. Once task-related electrophysiological signatures are identified, it will be important to explore recurrences of task-related neural states in non-task locked, real-world behavior [35]. For example, if cognitive control signals are insufficient, stimulation amplitude could be increased to improve decision-making capacity [36–38].

Changing DBS parameters and electrode impedance over time will present challenges in neural data interpretation. Even relatively small changes in impedance have been proven to affect the spectral power distribution [39]. Further, variability in sensing and stimulating contact placement will likely lead to inconsistent neural activity across participants [40–42]. Here, all five subjects had the deepest portion of the leads anchored in gray matter (VS or BNST; Figure 2 and Extended Data Figure 1). The stimulation contacts were the second deepest contact on the lead, flanked by sensing contacts. Therefore, the deepest sensing contact in each bipolar pair is likely sensing neural activity from gray matter, whereas the other contact in the pair is likely sensing neural activity from white matter. LFP from pure white matter is notoriously difficult to interpret [43], however it is unknown how heavily influenced the recorded voltages are by gray and white matter VS activity. Nevertheless, the gray-white bipolar sensing contact pairs undoubtedly lead to caveats in interpretation of our neural recordings.

The DBS implants used in our study allow for real-time frequency-domain analysis of electrophysiological activity recorded simultaneously during stimulation delivery from the implanted electrodes [20]. If a reliable relationship between patient state (severity of symptoms or adverse effects) and electrophysiology can be determined, computational methods can produce a classifier that identifies subject state based on measured activity. 'Untethered', embedded aDBS solutions are limited by onboard feature estimation and classification capabilities. For example, when embedded on an implanted device, the device can adjust its output based on LFP spectral power in predefined spectral bands used as inputs to a linear discriminant classifier [20]. While we observed correlations between power in various frequency bands and OCD symptom intensity, additional data collection and analysis is required to validate this finding in a larger sample. As putative biomarkers are identified, further work will be necessary to determine if biomarker-controlled adjustments in stimulation parameters result in an increased therapeutic effect of DBS.

Evidence from tractographic and functional imaging studies suggests that the pathophysiology of OCD does not lie in the VC/VS alone, but rather in the cortico-striatal-thalamo-cortical (CSTC) network [44,45]. One frontrunning hypothesis is that DBS acts to disrupt pathological frontostriatal hyperconnectivity in OCD. Several studies, via functional imaging [46] and intracranial electrophysiology [47], have shown evidence toward this hypothesis. Few studies report on oscillatory activity in the VC/VS to date, including in cohorts of patients with obesity [48], addiction [49], treatment resistant depression (TRD) [50,51], and OCD [51–54]. While there is no convergence on an oscillatory biomarker of OCD symptoms across these studies, there is promising evidence that VC/VS oscillatory activity may be correlated with behaviors including reward anticipation [48,50], error monitoring [49], OCD symptom provocation [52,54]. Chronic, ecologically valid, VC/VS recordings in humans may provide opportunities to identify a robust candidate biomarker for OCD symptoms.

For our approach to be optimally useful in treatment of obsessive-compulsive symptoms, we must better understand frontostriatal network activity. Obsessive-compulsive behaviors implicate symptomatic networks. OCD stimulation targets are anatomically linked to structures including the orbitofrontal cortex, the anterior cingulate cortex, the mediodorsal thalamic nucleus, and the ventral pallidum [44,45,55,56]. Stimulation to these targets impacts distributed network-wide activity and has been found to restore frontostriatal network activity in OCD [46]. Physiological studies point to relationships between frontostriatal activity and abnormal reward processing [40,57], cognitive flexibility[58], and decision making[59]; mental processes related to OCD symptoms. Further, connectivity with the prefrontal cortex/supplementary motor area has been shown to be correlated with improvement in OCD symptoms [47,53,60]. This literature supports the notion that symptoms arise from network phenomena and motivates the need for both cortical and subcortical inputs as well as simultaneous chronic, intracortical recordings to replicate findings in ecologically valid environments. To best understand the network, technical innovation must include the capacity to record in a few key areas in addition to the VC/VS, including the orbitofrontal cortex (OFC) or the anterior cingulate (ACC).

Finally, we note that the data collection platform presented here could be used in many other contexts beyond DBS programming sessions, daily activities at home, and ERP teletherapy for neuropsychiatric patients. To identify robust electrophysiological biomarkers for any psychiatric illness, data must be captured and explored for a vast array of behaviors and contexts. Wireless streaming of neural data enables capture of intracranial electrophysiology data during naturalistic states, including sleep, socialization, eating, and exercise. The platform presented here lays the groundwork for future transformational studies reliant on ecological neural and behavioral monitoring and assessment of neuropsychiatric illness.

Methods

Study design

An Early Feasibility Study of aDBS was conducted in adults with severe and intractable OCD (NCT04281134, NCT03457675). Subjects entered a 6-month trial of open-label bilateral DBS targeting the ventral capsule/ventral striatum (VC/VS) followed by 2 months of adjunctive exposure and response prevention therapy (ERP). Subsequently, they entered

a blinded discontinuation period to assess the need for ongoing DBS. The primary clinical outcome measure was change in the Yale-Brown Obsessive Compulsive Scale (Y-BOCS) scores, where a 35% reduction from baseline defined subjects as “responders”.

To date, five adult subjects with a principal diagnosis of severe and intractable OCD underwent DBS surgery after being apprised of the risks, possible benefits, and alternatives to participation in the research study. All subjects had OCD for more than five years and failed, or were unable to tolerate, adequate trials of multiple medications (i.e., selective serotonin reuptake inhibitors (SSRIs), clomipramine, and SSRI plus antipsychotics) and as well as a course of ERP. Two participants (P1: 31M and P2: 39F) were implanted with the Activa PC+S® (Medtronic, Minneapolis, MN, USA) device, and three participants (P3: 37F, P4: 40M, and P5: 31F) were implanted with the Summit RC+S® (Medtronic, Minneapolis, MN, USA) device. Each subject gave fully informed consent according to study sponsor guidelines, and all procedures were approved by the local institutional review board at Baylor College of Medicine (H-40255 and H-44941 to Baylor College of Medicine, IAA 17–27 and IAA 19–51 to Brown University, and STUDY20110082 and STUDY20110084 to University of Pittsburgh) and the US. Food and Drug Administration Center for Devices and Radiological Health. Subjects received a stipend after each study visit via a ClinCard.

DBS surgery

DBS leads (Model 3387) were placed bilaterally in the VC/VS region. Lead locations were determined using direct targeting on the preoperative magnetic resonance imaging (MRI): we targeted the gray-white interface in the ventral region of the anterior limb of the internal capsule. We created two trajectories per hemisphere, one immediately anterior and one immediately posterior to the anterior commissure (AC). We conceive of these targets not as different regions but rather as two anatomical methods to find the optimal, individual-specific target within the same “VC/VS region”, consistent with recent connectomic studies [44]. We refer to the anterior target as the “VC/VS” per se, as the VS is the gray matter immediately subjacent. We refer to the posterior target as the “BNST”, as the bed nucleus of the stria terminalis is immediately subjacent.

We used the observation of a “mirth” or “positive valence” response during intraoperative testing as an indicator of which location within the broader ventral capsule region will be more promising for eventual symptomatic improvement. Our decision to evaluate therapeutic response to DBS on both sides of the AC is driven by empirical evidence from the literature that more posterior targets lead to better outcomes. This effect may be related to the distribution of the passing fibers that fan out and diverge at the AC, which has been characterized via tractography and can vary for individual patients [44,45]. There is tractographic evidence that this positive mood response is due to DBS engagement of tracts that are more ventral, including the anterior cingulate cortex (ACC), OFC and ventromedial prefrontal cortex (vmPFC) [56]. We think of positive valence activation as a guidepost, as it may indicate that DBS is engaging the ventral limbic tracts that are associated with OCD.

The leads were connected to extensions, tunneled down the neck, and connected to the Activa PC+S® or Summit RC+S® placed in the upper left chest to enable wireless

streaming of Local Field Potential (LFP) data. P1, P3, P4, and P5 received bilateral stimulation, and P2 received unilateral stimulation.

Clinical assessments

The Y-BOCS and Yale-Brown Obsessive-Compulsive Scale II (Y-BOCS II) [61] were administered during clinical visits before DBS programming sessions. The Y-BOCS is the gold-standard clinician-administered tool for measuring severity of OCD and assessing treatment response [62,63]. The Y-BOCS II is a modified version of the original Y-BOCS that was designed to be more sensitive to changes in symptom severity among patients with very severe OCD [61].

MRI protocol

Preoperative magnetic resonance imaging (MRI) was performed on a Siemens Prisma 3T scanner (Erlangen, Germany) with a 64-channel head-neck coil. High resolution (0.8 mm isotropic) T1-weighted (T1w) anatomical images (MPRAGE; TR/TE/TI=2400/2.24/1000 ms, flip angle=8º, TA ~ 7 min) were acquired. T2-weighted (T2w) images (SPACE; 0.8mm isotropic; TR/TE = 3200/563ms, TA ~6min) were acquired in the same session.

CT imaging

In addition, the participants underwent preoperative clinical computerized tomography (CT) acquisition with contrast, as well as postoperative clinical CT acquisition to confirm electrode implant locations. The postoperative CT data were registered to the T1w MRI space and was used to extract the contact positions relative to local neuroanatomy.

Cortical reconstructions

An automatic cortical reconstruction was performed on the preoperative T1w MRI using FreeSurfer v7.1.1 (http://surfer.nmr.mgh.harvard.edu) [64] and the T2w MRI was used to improve reconstruction of the pial surfaces. The postoperative CT was aligned to the preoperative T1w MRI using the Functional Magnetic Resonance Imaging for the Brain Software Library's (FMRIB's) Linear Image Registration Tool (FLIRT) v6.0 [65,66]. Electrode coordinates were manually determined from the co-registered CT in BioImage Suite v3.5b1 [67] and placed into the native MRI space. The reconstructed cortical surface (pial surface), segmented subcortical structures, and electrode coordinates were visualized using the Multi-Modal Visualization Tool (MMVT) [68,69]. The caudate, putamen, and the ventral striatum were colored on the T1w slice based on the subcortical segmentation. Anterior Commissure (AC) was manually reconstructed by tracing the white fiber tracts on the T1w MRI slice.

Medtronic Summit RC+S® research platform

Herein, we concentrate on data gathered from the three subjects implanted with the Summit RC+S® system as it allows for extensive home recordings not possible with the Activa PC+S® system. The Summit RC+S® implanted neural stimulator (INS) enables both neurostimulation and continuous telemetry of intracranial LFP and accelerometry. The Clinician Telemetry Module (CTM) enables bi-directional communication between the INS (via telemetry) and a custom-built application developed with the Research Development Kit

(RDK) (via bluetooth to a separate host computer). The SurfacePro and SurfaceGo tablets were used in the clinic and at home to deploy the custom-built clinician and patient-facing applications that interface with the INS and cloud (Box.com) to create a flexible platform for data collection and storage. During recording sessions, the CTM must be within arm's reach (1 m) of the INS, and the host computer must be within the same room.

Summit RC+S® DBS programming session protocol

Summit RC+S® recordings during DBS programming sessions in the clinic were conducted using a clinician-facing application that communicates with the Medtronic Summit Application Programming Interface (API) running on a Surface Pro tablet (https://github.com/openmind-consortium/App-aDBS-ResearchFacingApp). The application allows for changes in bipolar sensing contact configuration, stimulation groups, and stimulation parameters including amplitude, pulse width, and rate within previously defined safe boundaries set by the clinician using the Medtronic Research Lab Programmer (RLP). Starting a recording session triggered sensing from two LFP channels and xyz acceleration.

DBS parameter optimization is completed solely on the basis of clinical evaluation, including standardized clinical assessments (e.g., Y-BOCS), interactions with subject and family members, and subjective patient reports of changes in mood, anxiety, alertness during acute DBS programming. To determine optimal stimulation parameters, the clinician adjusted one stimulation parameter at a time (either amplitude or pulse width), pausing to assess the participant's mood and symptoms after each change.

In addition to Summit RC+S® recordings, additional multi-modal electrophysiological recordings were conducted simultaneously during DBS programming sessions. These recordings include video of the face to enable (AFAR) and estimation of head velocity, electroencephalography (EEG), electrocardiogram (ECG), and blood volume pulse (BVP), and are further described in the sections below.

At-home recording session protocol

Study participants implanted with the RC+S® (P3, P4, and P5) agreed to participate in electrophysiological recordings, momentary self-report behavioral assessments, and behavioral tasks in their home environments.

Participants started their own recording sessions using a patient-facing application (frontend: https://github.com/openmind-consortium/App-OCD-PatientFrontend, backend: https://github.com/openmind-consortium/App-OCD-PatientBackend) that communicates with the Medtronic Summit API. To start a recording, the participant opened the application, and pressed a button on the User Interface labeled 'Record'. Pressing the 'Record' button triggered sensing from two LFP channels and xyz acceleration. Stimulation parameters were constant throughout each recording at home. The StriveStudy mobile application was also used to collect heart rate and acceleration data via an Apple Watch.

Protocol for the three different types of recordings the participants were asked to complete at home (daily recordings, task recordings, and sprint recordings) is further described below.

Daily recordings

Participants were asked to do at least one 30-minute recording session per day during unstructured daily activities at home, with one day off each week. Before each recording session, participants were asked to complete a momentary self-report behavioral assessment.

Momentary self-report behavioral assessments

Participants used the Rune Labs StriveStudy mobile application (Rune Labs Inc., San Francisco, CA) to report their OCD symptom intensity on a scale from zero to 10, where zero corresponds to 'very slightly or not at all', five corresponds to 'moderately', and 10 corresponds to 'extreme.' Due to the highly yoked nature of obsessive-compulsive symptoms, OCD symptom intensity ratings did not distinguish between obsessions and compulsions. The Rune Labs mobile application was deployed at zero weeks since DBS ON in P3, 13 weeks since DBS ON in P4, and 4 weeks before DBS ON in P5.

Task recordings

Participants were asked to complete behavioral tasks during a recording session one time each week. Behavioral tasks include the Multi-Source Interference task for assessing cognitive control and cognitive flexibility (https://github.com/brown-ccv/task-msit) [70,71], the Beads task for assessing intolerance to uncertainty and sensitivity to reward adapted from Voon et. al [72], and the Resting State task to gauge brain activity at rest (https://github.com/brown-ccv/task-resting-state). Tasks were all developed using Honeycomb, a template for reproducible behavioral tasks for clinic, laboratory, and home use (https://github.com/brown-ccv/honeycomb) [28]. Honeycomb allows for flexible task deployment with and without external electrophysiological recordings, and enables our experiments in both research settings and at home.

Sprint recordings

Participants were asked to engage in multi-day 'sprint' recording (i.e., multi-hour recording sessions). During the sprint recordings, participants were asked to use the StriveStudy mobile application to report their OCD symptom intensity on an hourly basis.

Exposure and Response Prevention therapy recordings

Participants engaged in a course of ERP teletherapy (13 to 14 appointments) from approximately 10 to 12 months after DBS was turned on. Participants were asked to start a recording session at the beginning of the appointment, and video recordings were saved to the clinician's computer using Zoom Video Communications (San Jose, CA, USA).

Local field potential recordings

LFPs were sampled at a rate of 200 Hz (Activa PC+S®) or 1000 Hz (Summit RC+S®) in the clinic, and 250 Hz (Summit RC+S®) at home. LFPs were sensed in bipolar configuration, meaning that a pair of sensing contacts was selected on each lead so that the signal recorded by one sensing contact is referenced to the other in the pair. Sensing and stimulation contact information for each participant is provided in Extended Data Table 1. To reduce DBS-related artifacts, the sensing contact pair was configured to flank the

stimulation contact when possible. The low pass filter stage 1 and 2 cut-off frequencies were both set to 100 Hz to further minimize impact of stimulation artifact on the recorded signal. The high pass filter cut-off frequency was set to 0.85 Hz. All sensing was conducted using active recharge stimulation. Acceleration in the x, y, and z axes was also measured onboard the Summit RC+S® device by an accelerometer located in the case.

Electroencephalography and peripheral electrophysiology recordings

Electroencephalography (EEG) was recorded during programming sessions and behavioral tasks in the clinic using a 64-channel active-electrode cap (actiCAP slim, Brain Products GmbH, Munich, Germany) and amplifiers (BrainAmp MR Plus) with an online reference at electrode FCz. Event markers were recorded along with EEG data using a TriggerBox (Brain Products GmbH) as well as a photodiode. EEG data was sampled at 5 kHz with a high cutoff at 1000 Hz using BrainVision Recorder. Three-lead electrocardiogram (ECG) and Blood Volume Pressure (BVP) were connected to the BrainAmp ExG amplifier. ECG leads were connected to just above and below the left pectorals, grounded to below the right pectoral. The BVP sensor was clipped onto the index finger of the non-dominant hand.

Audio and video recordings

Video and audio were recorded using the GoPro Hero 6 (GoPro, San Mateo, CA, USA) at 25 fps, and an external microphone (Zoom H4n Pro 4-Track Portable Recorder, Zoom Corporation, Tokyo, Japan) at 44.1 kHz. High quality audio was synchronized with video by cross correlating the low and high quality audio tracks recorded by the GoPro Hero 6 and external microphone, respectively. Then the original audio was removed from the video and replaced by the high quality audio.

Remote data management

Data from the Summit RC+S® patient-facing application and behavioral task data was automatically uploaded to Box.com from SurfaceGo tablets via a .BAT script triggered by Windows Task Scheduler upon connecting to the internet, or user login/logout (https://github.com/neuromotion/rcps-box-upload).

Data synchronization: EEG to LFP

LFP and EEG data were synchronized by identifying features common to both recordings. Sequences of 5 Hz pulses were briefly applied at the beginning and end of each recording session. These pulses are visible in both the LFP and EEG recordings due to the high amplitude of the stimulation artifacts they produce. Corresponding pulses were identified in both recordings and used as alignment points.

Data synchronization: EEG to task (in-clinic)

The start and end time of DBS programming sessions were marked in the EEG recording using a “pseudo-behavioral task” consisting solely of a start/stop button. Pressing the start and stop button in the task triggered a serial event message that was sent from the SurfacePro tablet to the Brain Vision EEG amplifier via the TriggerBox.

Data synchronization: EEG to video

The pseudo-behavioral task also triggered a unique audible tone at the same time the serial event was sent. This tone was recorded by both the GoPro video camera and external microphone. The tone was identified algorithmically in each audio file using the Matlab function *findsignal*, and the time point of the tone was used as the synchronization point between audio/video and EEG recordings.

Data synchronization: Intracranial Electrophysiology to task (at-home)

Each behavioral task outputs a .JSON file containing data saved from the task including the Unix time (time of day) when each task event occurred. Task behavior and LFP were timestamped using the same clock (SurfaceGo clock), and therefore could easily be aligned.

Data synchronization: Intracranial Electrophysiology to Rune StriveStudy mobile application output

LFP Unix time was aligned to OCD symptom intensity rating, Apple Watch acceleration, and Apple Watch heart rate unix time.

Data synchronization: Intracranial Electrophysiology to ERP video

ERP video recordings were saved with a date and timestamp on each video frame. Time of day from the video was used to align video to LFP Unix time.

Signal reconstruction after packet loss

We accounted for packet losses in LFP data to enable synchronization between LFP and other data streams[73]. Details and code for the procedure we used is available at https://github.com/openmind-consortium/Analysis-rcs-data.

Artifact removal: low pass filter

Prior to filtering, missing LFP samples were replaced with the mean value of the remaining samples. LFP and EEG were then low-pass filtered using an FIR filter between 100 and 130 Hz with 40 dB of attenuation in the stopband and 0.1 dB of passband ripple. The filter was designed using the Matlab function *designfilt* and applied to the recording using *filtfilt*.

Objective, automatic measurement of affective valence and head dynamics

Facial expression of positive and negative valence and the dynamics of head motion were measured using Automated Facial Affect Recognition (AFAR). AFAR is a computer-vision based approach that can objectively measure the occurrence, intensity, and timing of facial action units [26,74–76], head pose [77] and gaze [78] at video frame rate (30 to 60 fps). Action units are anatomically based actions that individually or in combination can describe nearly all-possible facial expressions [79]. Previous research has identified action units associated with positive (e.g., enjoyment) and negative (e.g., fear, anger, disgust, and anxiety) emotion [80–82]; and representations of positive and negative valence and pain [83–86]. Velocity of head motion has been found to increase with strong negative affect [87–90] and is inversely related to severity of depression [91,92]. In preliminary studies, AFAR revealed strong effects of DBS in both intraoperative contexts and interviews [93,94].

We measured positive valence on a zero to five scale as the mean intensity of facial action units (AU) 6 and 12. AU 6 (*orbicularis oculi pars orbitalis*) raises the cheeks, narrows the eye aperture laterally, and can cause crows-feet wrinkles at the eye corners. AU 12 (*zygomatic major*) stretches the lips obliquely and affects shape and appearance of the nasolabial furrows. Head movements are measured by the angular velocity of pitch and yaw head motions in units of degree per second. Head pitch and yaw were smoothed using a five-second moving average before calculating frame-to-frame velocity. To aid interpretation, the frame-level velocity was converted to degrees per second. An example of AFAR tracking of positive valence and head velocity is shown in Figure 3B and C. Participants P4, P5, and author (A.D.W.) gave informed consent for publication of their images and videos in this manuscript.

Neural data analysis for sprint and ERP recordings at home

We analyzed one sprint dataset collected at home over multiple days by P4, 531–533 days after DBS surgery. We chose this dataset due to the high variability and large range in self-reported OCD symptom intensity ratings over the three day span. Our goal was to characterize how the spectral content of the VC/VS LFP signal was changing with OCD symptom intensity rating.

A total of 41 OCD symptom intensity ratings were reported during LFP recordings over the three-day span. LFP data were divided into two minute segments; one minute before and one minute after each self-reported OCD symptom intensity rating was logged. Within that time frame, all contiguous segments of data with a duration of 500 ms or more were included in analysis. A Hamming window (Matlab: *hamming*) was used to divide the data into 500 ms segments with 250 ms of overlap, and the mean of the entire recording was subtracted from each window to remove DC offset. Power Spectral Density (PSD) estimates were calculated using the Welch method (Matlab: *pwelch*). The median PSD was computed for each two minute segment. Transient outliers due to motion or background device processes were not explicitly removed but were handled by our choice of using median for central tendency. The median PSD was normalized by dividing by the average power between four and 80 Hz.

We then calculated average power in predefined frequency bands of interest (Delta: 0–4 Hz, Theta: 4–8 Hz, Alpha: 8–15 Hz, Beta: 15–30 Hz, and Gamma 30–55 Hz) by computing the mean power within each frequency band. Resulting values in [mV^2/Hz] were converted to decibels, [dB], by computing ten times the base ten logarithmic transform. Therefore, each OCD symptom intensity rating was associated with normalized average power in each predefined frequency band of interest. A line of least squares was fit to each scatter plot (Matlab: *lsline*) and the coefficient of correlation (R) was computed to measure the strength of the relationship between spectral band power and OCD symptom intensity rating.

Neural data analysis for ERP recordings at home

We repeated the analysis described in the previous section using one ERP dataset for each participant. The datasets chosen were 232 days after surgery for P3, 278 days after surgery for P4, and 281 days after surgery for P5.

Extended Data

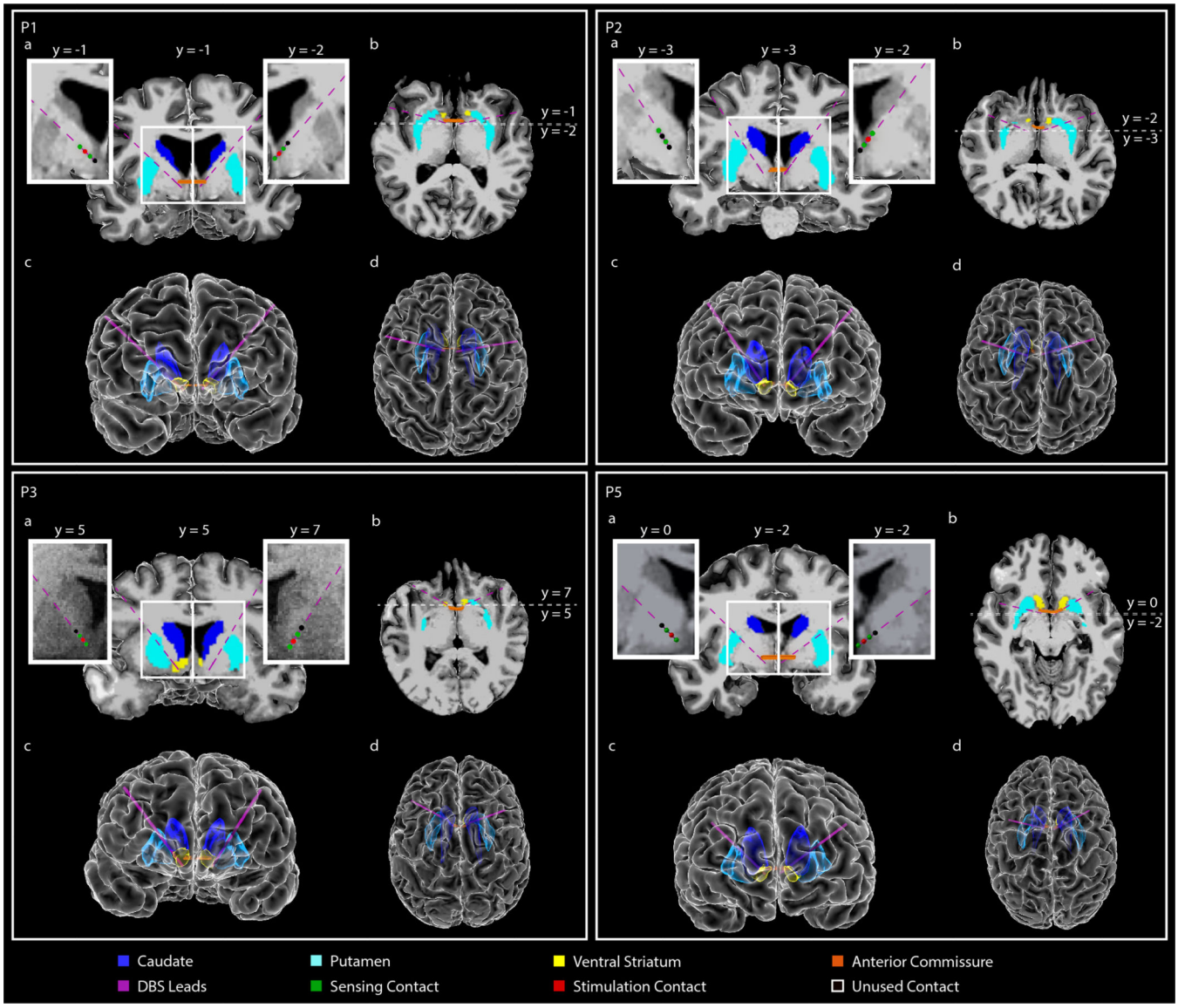

Extended Data Fig. 1 |. Anatomical localization of DBS lead placement (P1, P2, P3, P5).
(A,B) Coronal (A) and axial (B) T1-weighted (T1w) MRI in radiographic convention from participants P1, P2, P3, and P5 overlaid with reconstructed DBS lead trajectories. Colored regions indicate anterior commissure (AC), caudate, putamen, and ventral striatum (VS). The MRI slice shown is immediately posterior (A; coronal) or inferior (B; axial) to the most ventral contact. Enlarged coronal slices (corresponding to white box outlines in panel A) showing DBS contact locations in each hemisphere are shown on either side of the full coronal slice. Green spheres indicate sensing contacts, red spheres indicate stimulating contacts, black spheres indicate contacts that were used for neither stimulation nor sensing. In each participant, the tips of the leads were targeted to either the VS or the bed nucleus of the stria terminalis (BNST) (target regions for each participant are included in Table 1). Enlarged slices shown are immediately posterior to the most ventral contact

in each hemisphere. Anterior-posterior slice location (*y*) is referenced to the posterior border of the AC, which is defined as *y*=0. (D,E) Front (D) and top-down (E) view of the reconstructed cortical surface, subcortical structures, DBS leads, and AC, shown in radiographic convention.

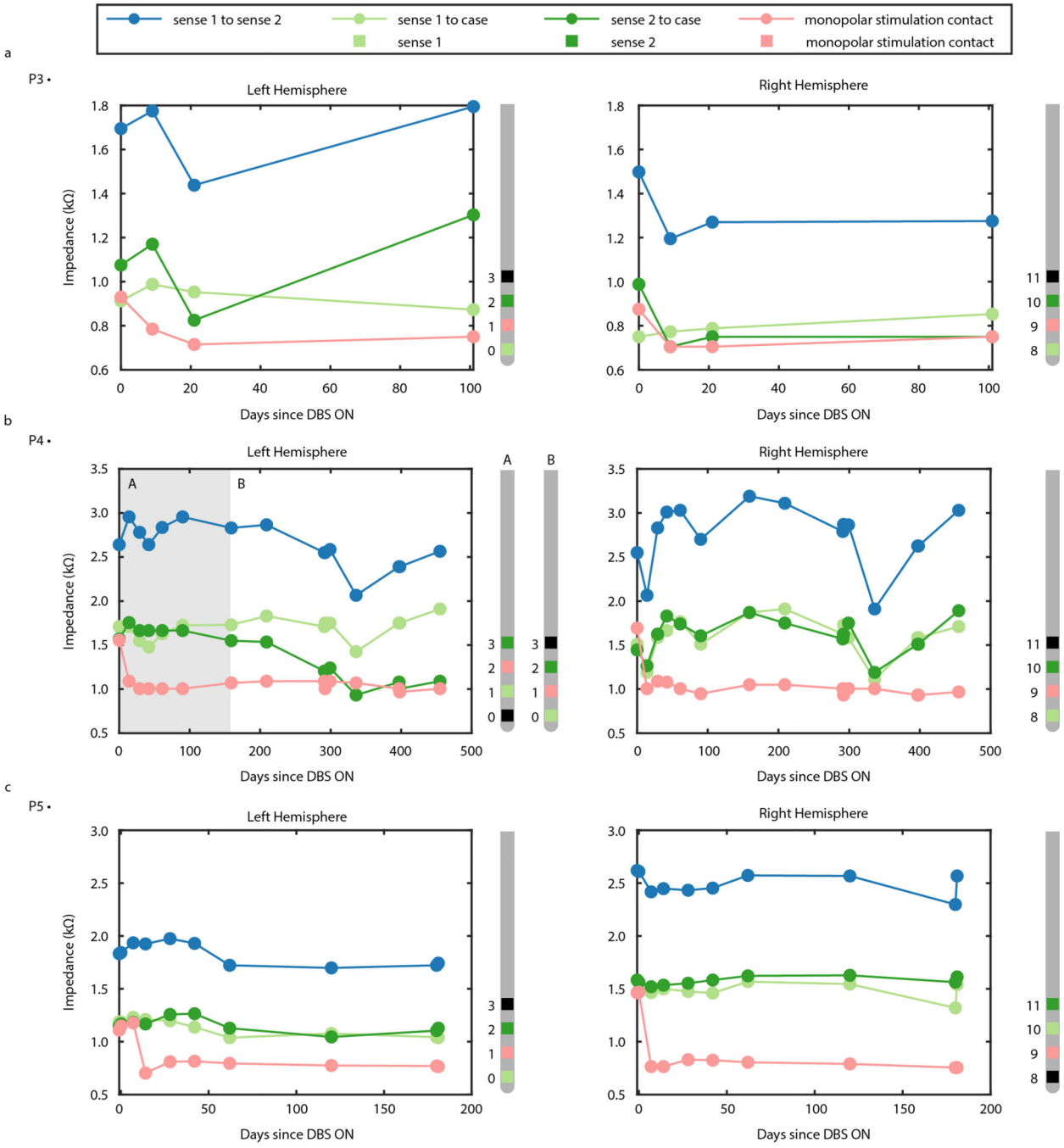

Extended Data Fig. 2 |. Impedance of sensing and stimulation electrode contacts reflect long term stability at device-tissue interface.

(A) Impedance in kOhms of sensing and stimulation electrode contacts in the left (left panel) and right (right panel) VC/VS of P3. Blue points indicate impedance between the

two sensing contacts. Green points indicate the impedance between the deepest (light green) and shallowest (dark green) sensing contact and the INS case. Light red points indicate the impedance between the stimulation contact and the INS case. Sense and stimulation electrode contacts on the Medtronic 3387 leads are visualized to the right of each panel, with contact 0 as the deepest contact on the left, and contact 8 as the deepest contact on the right. Light green indicates the deepest sensing contact, Green indicates the shallowest sensing contact, and light red indicates the stimulation contact. Black contacts are unused. (B) Impedance in kOhms of sensing and stimulation electrode contacts in the left (left panel) and right (right panel) VC/VS of P4. Gray shaded region indicates the timespan when sensing and stimulation contacts correspond to the Medtronic 3387 lead diagram labelled with “A”, whereas the following timespan with no shading corresponds to the Medtronic 3387 lead diagram labelled with “B”. Elsewise, the format is identical to panel A. (C) Impedance in kOhms of sensing and stimulation electrode contacts in the left (left panel) and right (right panel) VC/VS of P5. Format is identical to panel A.

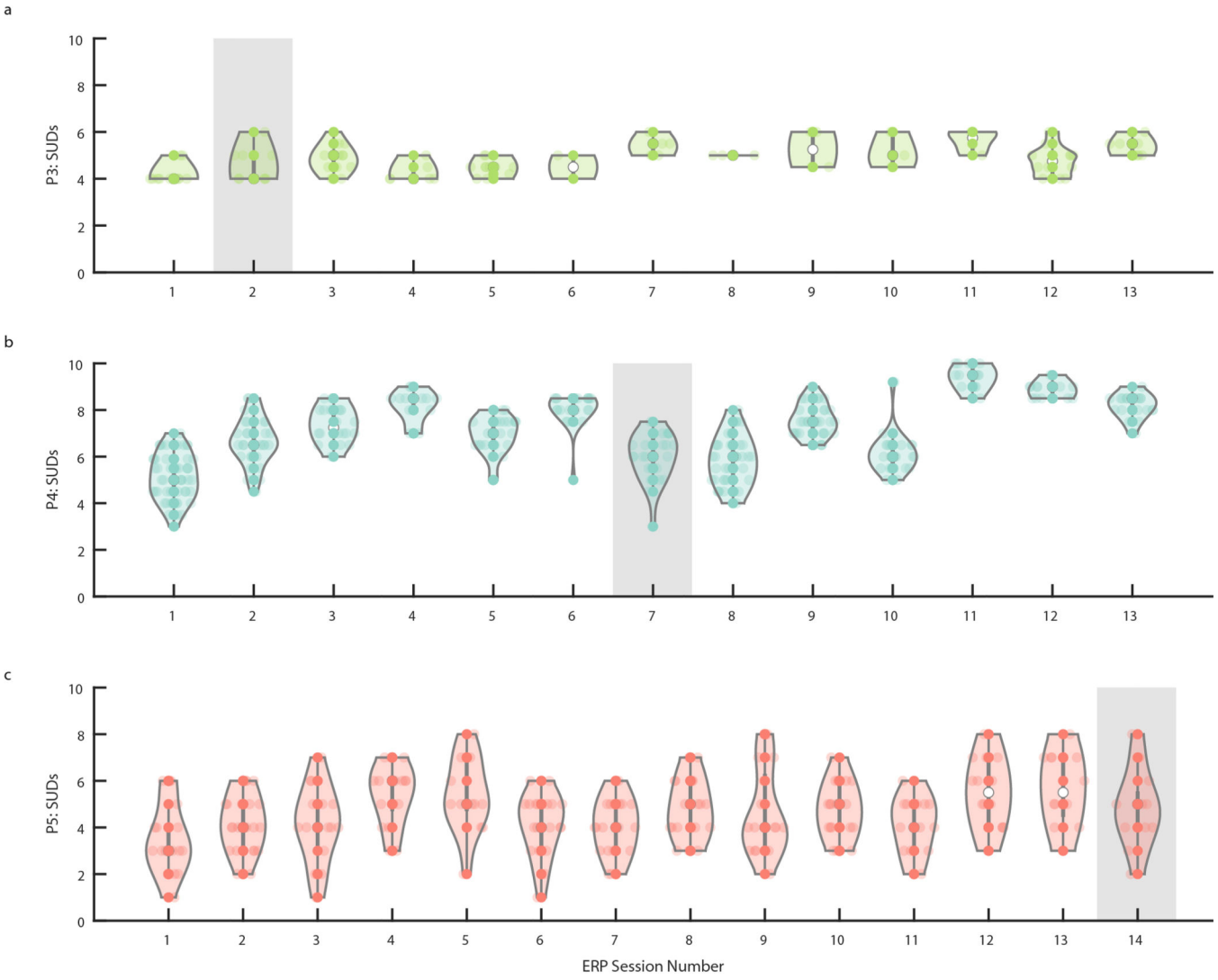

Extended Data Fig. 3 |. Distribution of self-reported, Subjective Units of Distress (SUDs) ratings collected by participants during Exposure Response Prevention (ERP) teletherapy.

(A) The distribution of SUDs ratings by participant P3 for all recorded sessions. The *Y-axis* shows SUDs ratings provided by the participant after being prompted to indicate their level of OCD related distress at irregular time intervals during each ERP session on a scale of 0–10 with 0 representing 'no distress' and 10 representing 'the worst distress.' The *X-Axis* shows each consecutive, hour-long, recorded ERP session (n=13 to n=14 for each participant) completed. Gray shading indicates the session analyzed in Extended Data Fig. 6. (B) The distribution of SUDs ratings by participant P4 for all recorded sessions. Format is identical to panel A. Gray shading indicates the session analyzed in Extended Data Fig. 7. (C) The distribution of SUDs ratings by participant P5 for all recorded sessions. Format is identical to panel A. Gray shading indicates the session analyzed in Extended Data Fig. 8.

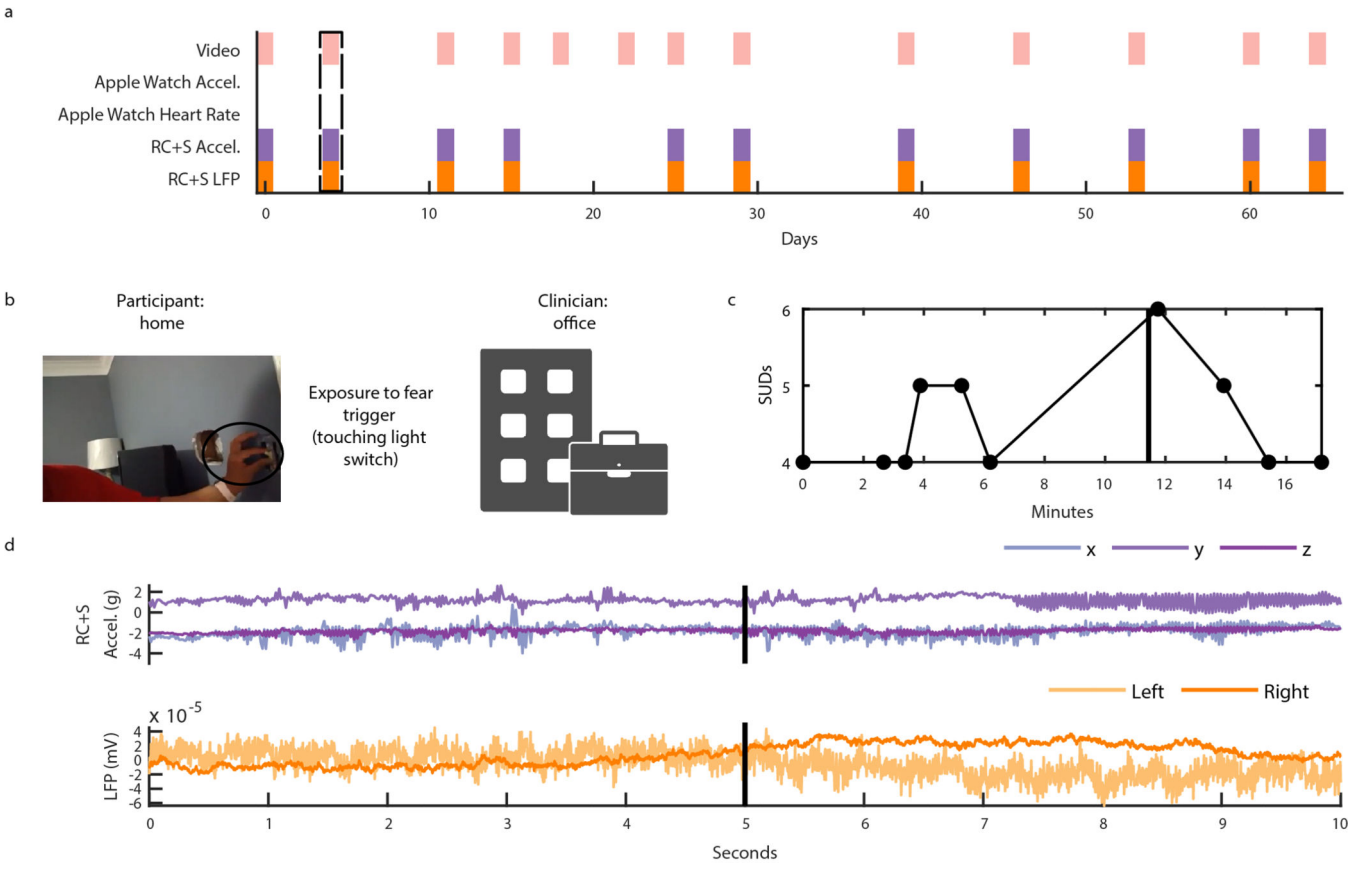

Extended Data Fig. 4 |. Intracranial electrophysiology during Exposure and Response Prevention (ERP) teletherapy at home with Participant P3.

(A) Calendar availability plot of ERP sessions for participant P4, over days since the first ERP session. Shaded portions indicate data availability for ERP video, Apple watch heart rate, Apple watch acceleration, RC+S acceleration, and RC+S LFP. Rectangular dotted line corresponds to the ERP session example data shown in panels B-D. (B) Video of participant P4 (left), clinician (right). (C) Time-course in minutes of self-reported Subjective Units of Distress (SUDs) ratings. Vertical black line corresponds to the video frame shown in panel B. (D) Ten seconds of example data synchronized to video, including RC+S acceleration,

and two bipolar LFP channels. Vertical black line corresponds to the video frame shown in panel B.

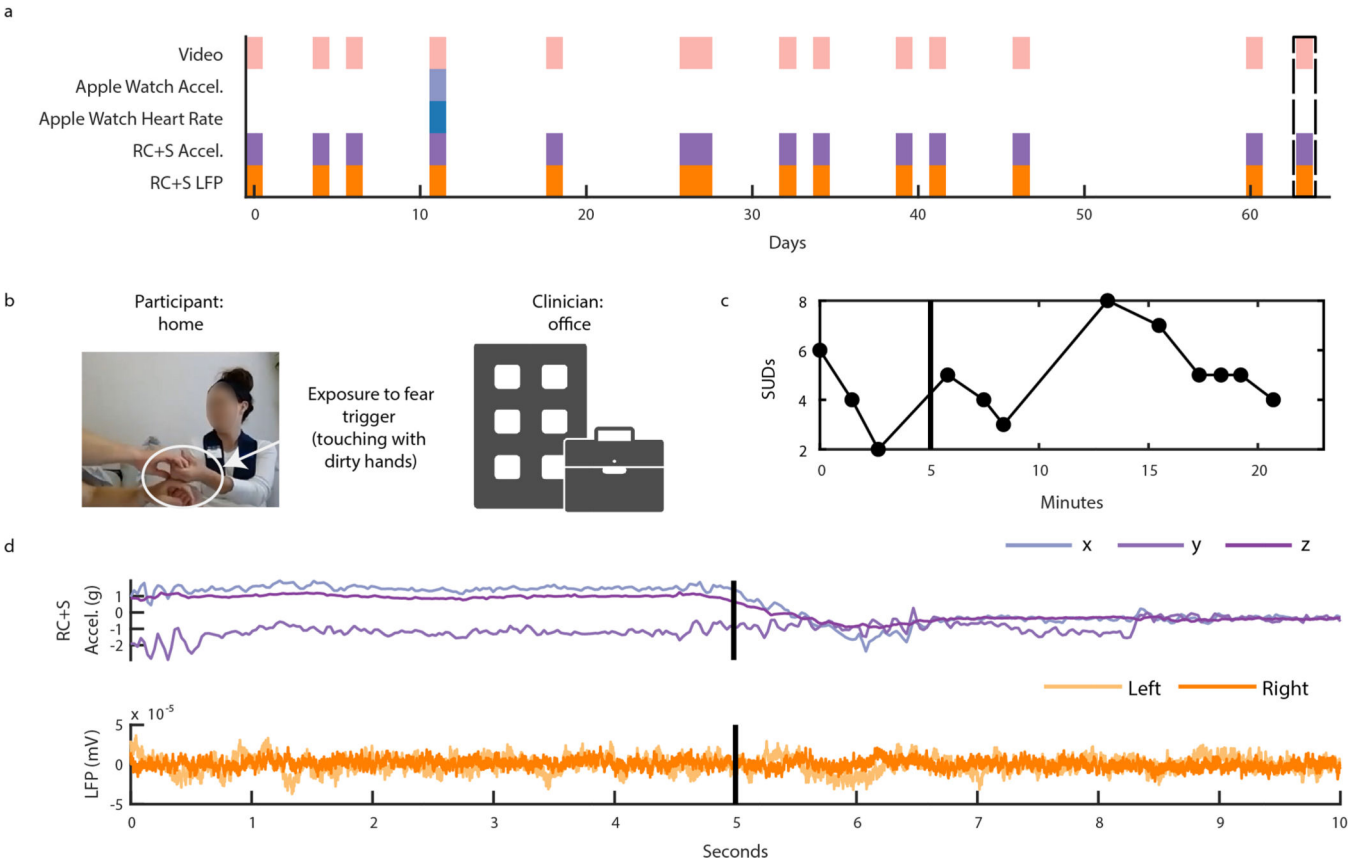

Extended Data Fig. 5 |. Intracranial electrophysiology during Exposure and Response Prevention (ERP) teletherapy at home with Participant P5.

(A) Calendar availability plot of ERP sessions for participant P4, over days since the first ERP session. Shaded portions indicate data availability for ERP video, Apple watch heart rate, Apple watch acceleration, RC+S acceleration, and RC+S LFP. Rectangular dotted line corresponds to the ERP session example data shown in panels B-D. (B) Video of participant P4 (left), clinician (right). (C) Time-course in minutes of self-reported Subjective Units of Distress (SUDs) ratings. Vertical black line corresponds to the video frame shown in panel B. (D) Ten seconds of example data synchronized to video, including RC+S acceleration, and two bipolar LFP channels. Vertical black line corresponds to the video frame shown in panel B.

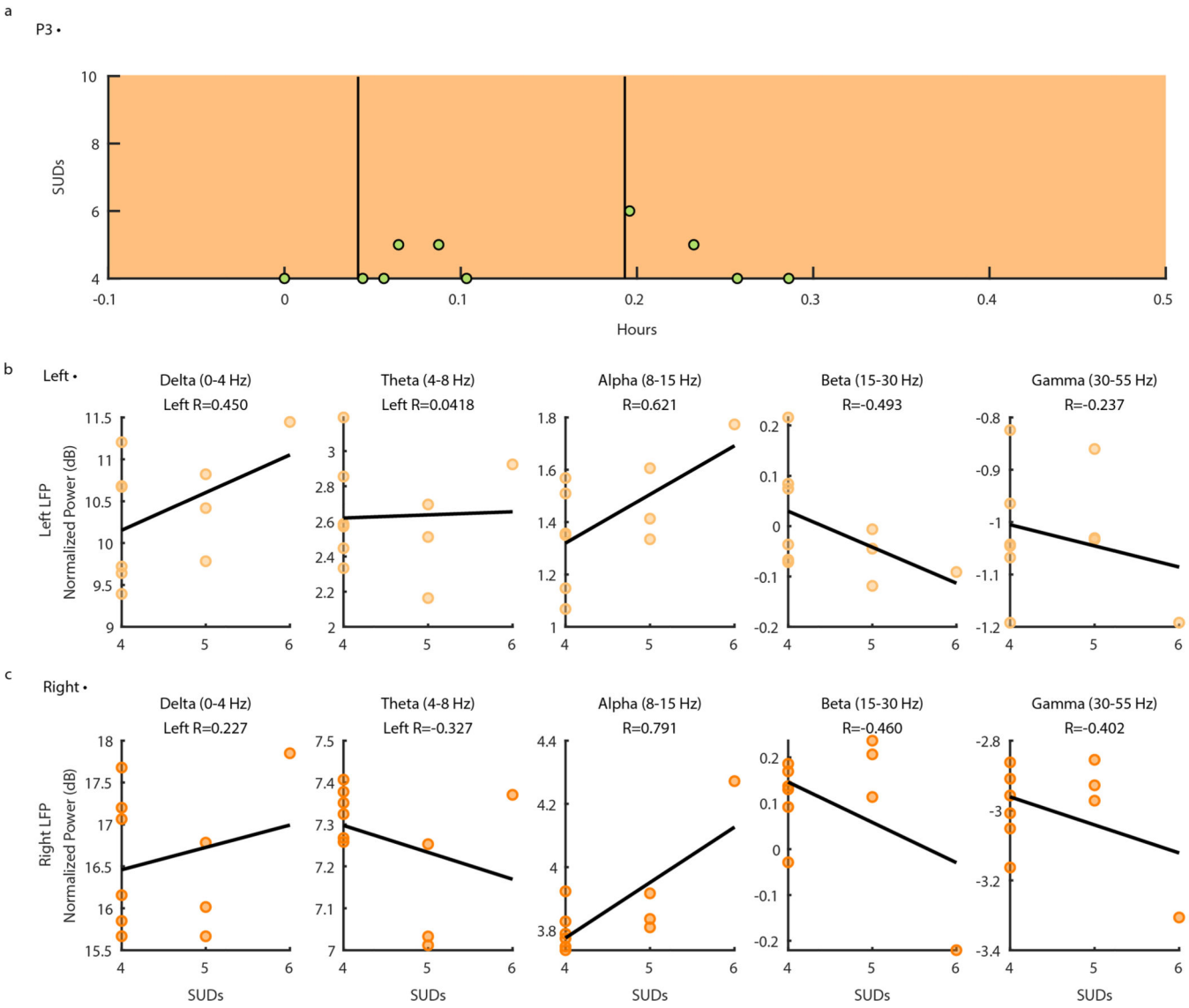

Extended Data Fig. 6 |. Ventral Capsule/Ventral Striatum spectral activity vs. SUDs ratings during P3 Exposure and Response Prevention (ERP) teletherapy recording.

(A) Self-reported intensity of OCD symptoms (scatter points) shown over time in hours with LFP data availability (orange shading). Vertical black lines indicate timepoints of OCD exposures. B) Normalized left VC/VS spectral power in Delta (0–4 Hz), Theta (4–8 Hz), Alpha (8–15 Hz), Beta (15–30 Hz), and Gamma (30–55 Hz) (from left to right) vs. self-reported OCD symptom intensity from zero to 10. Black lines represent the line of least squares. R values correspond to the coefficient of correlation. (C) Normalized right VC/VS spectral power in frequency bands of interest vs. self-reported OCD symptom intensity from zero to 10. Format is identical to panel B.

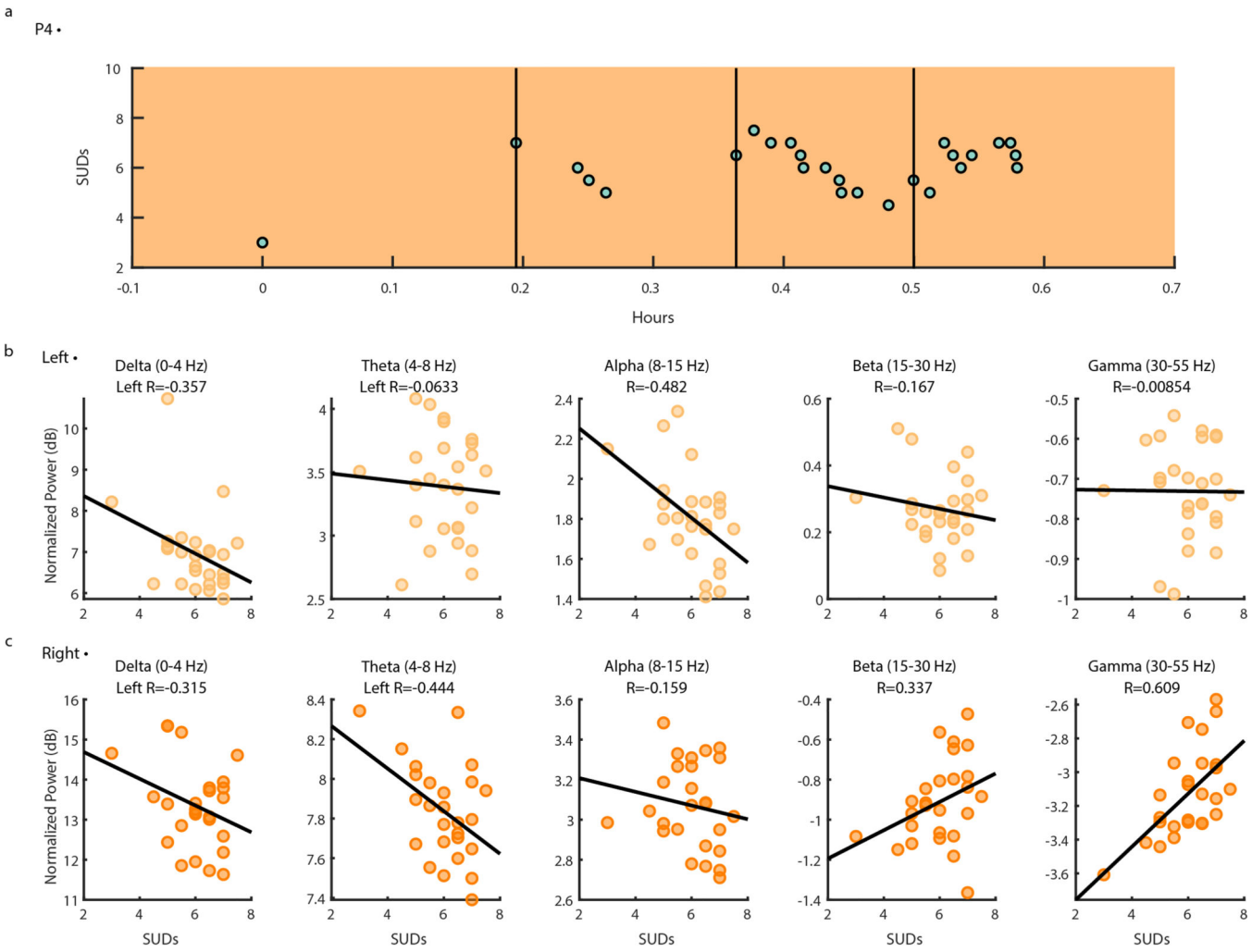

Extended Data Fig. 7 |. Ventral Capsule/Ventral Striatum spectral activity vs. SUDs ratings during P4 Exposure and Response Prevention teletherapy recording.

(A) Self-reported intensity of OCD symptoms (scatter points) shown over time in hours with LFP data availability (orange shading). Vertical black lines indicate timepoints of OCD exposures. B) Normalized left VC/VS spectral power in Delta (0–4 Hz), Theta (4–8 Hz), Alpha (8–15 Hz), Beta (15–30 Hz), and Gamma (30–55 Hz) (from left to right) vs. self-reported OCD symptom intensity from zero to 10. Black lines represent the line of least squares. R values correspond to the coefficient of correlation. (C) Normalized right VC/VS spectral power in frequency bands of interest vs. self-reported OCD symptom intensity from zero to 10. Format is identical to panel B.

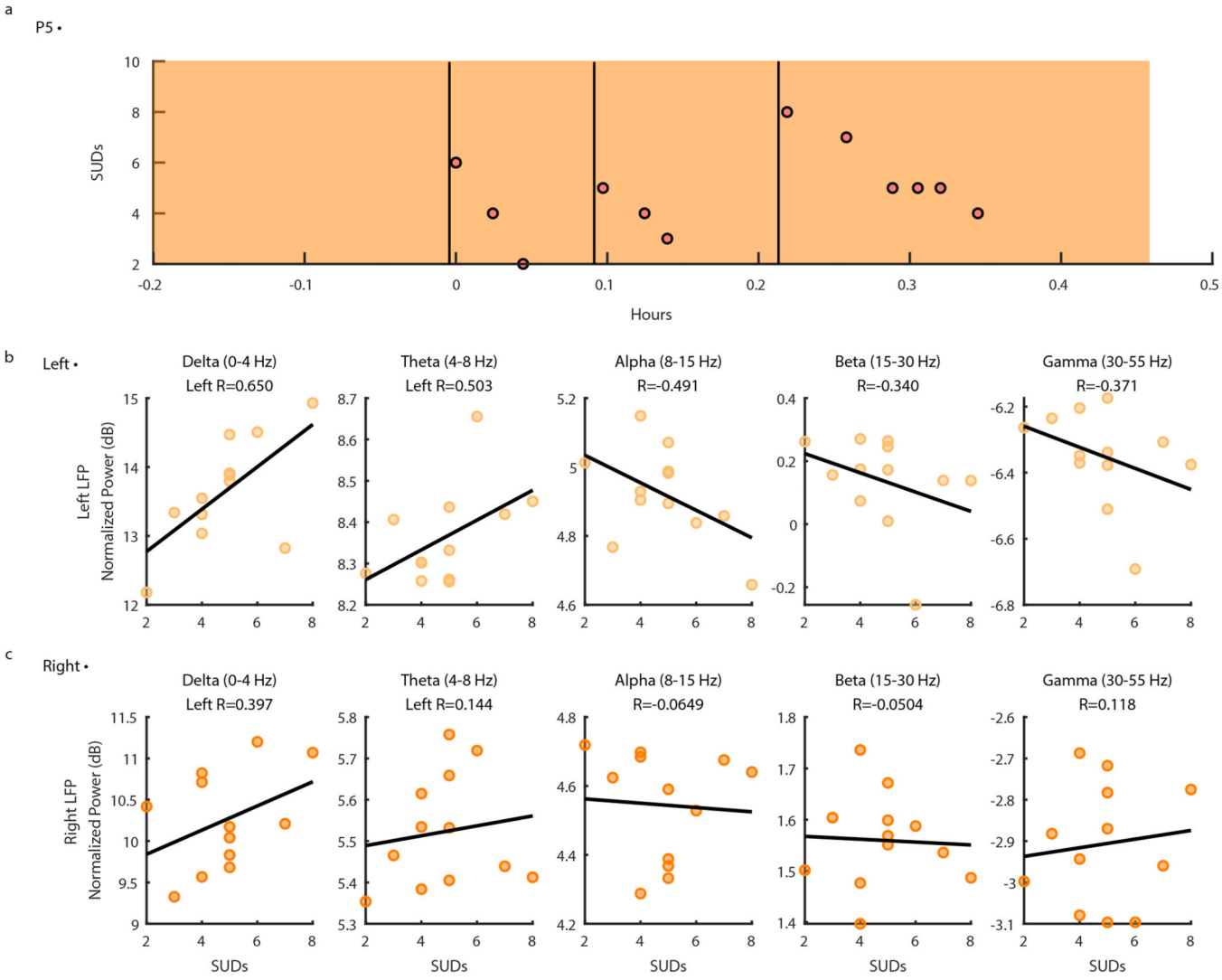

Extended Data Fig. 8 |. Ventral Capsule/Ventral Striatum spectral activity vs. SUDs ratings during P5 Exposure and Response Prevention teletherapy recording.

(A) Self-reported intensity of OCD symptoms (scatter points) shown over time in hours with LFP data availability (orange shading). Vertical black lines indicate timepoints of OCD exposures. B) Normalized left VC/VS spectral power in Delta (0–4 Hz), Theta (4–8 Hz), Alpha (8–15 Hz), Beta (15–30 Hz), and Gamma (30–55 Hz) (from left to right) vs. self-reported OCD symptom intensity from zero to 10. Black lines represent the line of least squares. R values correspond to the coefficient of correlation. (C) Normalized right VC/VS spectral power in frequency bands of interest vs. self-reported OCD symptom intensity from zero to 10. Format is identical to panel B.

Extended Data Table 1 | Participant demographics, DBS surgery device and targets, and stimulation and sensing contact information.

MDD: Major Depressive Disorder, PTSD: Post-Traumatic Stress Disorder, GAD: General Anxiety Disorder, TS: Tourette's Syndrome., ET: Essential Tremor. *Responder = 35% or greater decrease in the Yale-Brown Obsessive-Compulsive Scale (Y-BOCS) after 12 months of activation compared to presurgical baseline. N/A refers to participants that have not completed study yet.

Participant:		P1	P2	P3	P4	P5
Gender		Male	Female	Female	Male	Female
Age at time of consent		31	39	37	40	31
Race		White	White	White	White	White
Ethnicity		Not Hispanic/ Latino	Hispanic/ Latino	Hispanic/ Latino	Not Hispanic/ Latino	Not Hispanic/ Latino
Primary diagnosis		OCD	OCD	OCD	OCD	OCD
Comorbid diagnoses		MDD	PTSD, MDD, GAD	PTSD, MDD, TS	Bipolar Disorder II	MDD
Principal OCD symptoms		Intrusive aggressive/ taboo obsessions with checking and repeating rituals	Intrusive aggressive/ sexual taboo obsessions with checking and repeating rituals	Intrusive aggressive thoughts, magical thinking, and scrupulosity with checking and repeating rituals	Contamination and scrupulosity obsessions with cleaning and checking rituals	Intrusive aggressive and contamination obsessions with checking and cleaning rituals
Age of OCD onset (years)		17	18	12	16	8
Responder status		Yes	Yes	Yes	Yes	Yes
Initial Y-BOCS II (Y-BOCS) score		37 (35)	39 (34)	46 (40)	42 (38)	47 (37)
Final Y-BOCS II (Y-BOCS) score		8(6)	11(9)	27 (25)	25 (22)	26 (23)
DBS Device		PC+S	PC+S	RC+S	RC+S	RC+S
DBS Target Region	L	BNST	BNST	VCVS	VCVS	BNST
	R	BNST	BNST	VCVS	BNST	BNST
Stimulating Contact	L	1−/C+	2−/C+	1−/C+	1 −/C+	1−/C+
	R	10−/C+	OFF	9−/C+	9−/C+	9−/C+
Sensing contact	L	0–2	1–3	0–2	0–2	0–2
	R	9–11	9–11	8–10	8–10	10–11
Final DBS Rate	L	150 Hz	150 Hz	150.6 Hz	150.6 Hz	150.6 Hz
	R	150 Hz	OFF	150.6 Hz	150.6 Hz	150.6 Hz
Final DBS Amplitude	L	5.0 V	5.5 V	6.0 mA	5.2 mA	6.0 mA
	R	5.0 V	OFF	5.7 mA	5.0 mA	6.0 mA
Final DBS Pulse Width	L	120 μs	120 μs	210 μs	120 μs	180 μs
	R	120 μs	OFF	210 μs	120 μs	180 μs

Supplementary Material

Refer to Web version on PubMed Central for supplementary material.

Acknowledgements:

The authors thank the participants and their families for their involvement in the research program. The authors also thank Kendall Lane for her artistic contribution in the creation of Figure 1. This work relied heavily on the community expertise and resources made available by the Open Mind Consortium (https://openmind-consortium.github.io). Summit RC+S® devices were donated by Medtronic as part of the BRAIN Initiative Public-Private Partnership Program (PPP). We thank John Murphy for his expertise and contributions in designing and machining equipment used in this study. Part of this research was conducted with the help of research staff at the Center for Computation and Visualization, Brown University (Senior Research Software Engineers Bradford Roarr, and Mary McGrath). The research was supported by the NIH NINDS BRAIN Initiative via contracts UH3NS100549 (SAS, JFC, DAB, EAS, WKG) and UH3NS103549 (SAS), the Charles Stark Draper Laboratory Fellowship (NRP), the McNair Foundation (SAS), the Texas Higher Education Coordinating Board, NIH 1RF1MH121371, U54-HD083092 (EAS), NIH MH096951 (JFC), K01-MH-116364 and R21-NS-104953 (KB), 3R25MH101076–05S2 (ABA), award 1S10OD025181 to Jerome Sanes at Brown University for computational resources, and the Karen T. Romer Undergraduate Teaching and Research Award at Brown University (EMDVR under guidance of DAB).

References

1. Goodman WK, Storch EA & Sheth SA Harmonizing the Neurobiology and Treatment of Obsessive-Compulsive Disorder. Am. J. Psychiatry 178, 17–29 (2021). [PubMed: 33384007]
2. Pallanti S, Hollander E. & Goodman WK A qualitative analysis of nonresponse: management of treatment-refractory obsessive-compulsive disorder. J. Clin. Psychiatry 65 Suppl 14, 6–10 (2004). [PubMed: 15554782]
3. Alonso P. et al. Deep Brain Stimulation for Obsessive-Compulsive Disorder: A Meta-Analysis of Treatment Outcome and Predictors of Response. PLoS One 10, e0133591 (2015). [PubMed: 26208305]
4. Goodman WK et al. Deep brain stimulation for intractable obsessive compulsive disorder: pilot study using a blinded, staggered-onset design. Biol. Psychiatry 67, 535–542 (2010). [PubMed: 20116047]
5. Ooms P. et al. Deep brain stimulation for obsessive-compulsive disorders: long-term analysis of quality of life. J. Neurol. Neurosurg. Psychiatry 85, 153–158 (2014). [PubMed: 23715912]
6. Denys D. et al. Efficacy of Deep Brain Stimulation of the Ventral Anterior Limb of the Internal Capsule for Refractory Obsessive-Compulsive Disorder: A Clinical Cohort of 70 Patients. Am. J. Psychiatry 177, 265–271 (2020). [PubMed: 31906709]
7. Okun MS & Foote KD Parkinson's disease DBS: what, when, who and why? The time has come to tailor DBS targets. Expert Review of Neurotherapeutics vol. 10 1847–1857 (2010). [PubMed: 21384698]
8. Angst J. et al. Obsessive-compulsive severity spectrum in the community: prevalence, comorbidity, and course. Eur. Arch. Psychiatry Clin. Neurosci. 254, 156–164 (2004). [PubMed: 15205969]
9. Graat I, Figee M. & Denys D. The application of deep brain stimulation in the treatment of psychiatric disorders. Int. Rev. Psychiatry 29, 178–190 (2017). [PubMed: 28523977]
10. Widge AS et al. Treating refractory mental illness with closed-loop brain stimulation: Progress towards a patient-specific transdiagnostic approach. Exp. Neurol. 287, 461–472 (2017). [PubMed: 27485972]
11. Provenza NR et al. The case for adaptive neuromodulation to treat severe intractable mental disorders. Front. Neurosci. 13, 152 (2019). [PubMed: 30890909]
12. Little S. et al. Bilateral adaptive deep brain stimulation is effective in Parkinson's disease. J. Neurol. Neurosurg. Psychiatry 87, 717–721 (2016). [PubMed: 26424898]
13. Swann NC et al. Adaptive deep brain stimulation for Parkinson's disease using motor cortex sensing. Journal of Neural Engineering vol. 15 046006 (2018).

14. Bergey GK et al. Long-term treatment with responsive brain stimulation in adults with refractory partial seizures. Neurology 84, 810–817 (2015). [PubMed: 25616485]
15. Opri E. et al. Chronic embedded cortico-thalamic closed-loop deep brain stimulation for the treatment of essential tremor. Sci. Transl. Med. 12, (2020).
16. Bouthour W. et al. Biomarkers for closed-loop deep brain stimulation in Parkinson disease and beyond. Nat. Rev. Neurol. 15, 343–352 (2019). [PubMed: 30936569]
17. Wingeier B. et al. Intra-operative STN DBS attenuates the prominent beta rhythm in the STN in Parkinson's disease. Exp. Neurol. 197, 244–251 (2006). [PubMed: 16289053]
18. Bijanki KR et al. Cingulum stimulation enhances positive affect and anxiolysis to facilitate awake craniotomy. J. Clin. Invest. 129, 1152–1166 (2019). [PubMed: 30589643]
19. Fullana MA et al. Diagnostic biomarkers for obsessive-compulsive disorder: A reasonable quest or ignis fatuus? Neurosci. Biobehav. Rev. 118, 504–513 (2020). [PubMed: 32866526]
20. Stanslaski S. et al. A chronically implantable neural coprocessor for investigating the treatment of neurological disorders. IEEE Trans. Biomed. Circuits Syst. 12, 1230–1245 (2018). [PubMed: 30418885]
21. Sun FT & Morrell MJ The RNS System: responsive cortical stimulation for the treatment of refractory partial epilepsy. Expert Rev. Med. Devices 11, 563–572 (2014). [PubMed: 25141960]
22. Kremen V. et al. Integrating Brain Implants With Local and Distributed Computing Devices: A Next Generation Epilepsy Management System. IEEE J Transl Eng Health Med 6, 2500112 (2018). [PubMed: 30310759]
23. Topalovic U. et al. Wireless Programmable Recording and Stimulation of Deep Brain Activity in Freely Moving Humans. Neuron 108, 322–334.e9 (2020). [PubMed: 32946744]
24. Gilron R. 'ee et al. Long-term wireless streaming of neural recordings for circuit discovery and adaptive stimulation in individuals with Parkinson's disease. Nat. Biotechnol. (2021) doi:10.1038/s41587-021-00897-5.
25. Storch EA et al. Defining clinical severity in adults with obsessive-compulsive disorder. Compr. Psychiatry 63, 30–35 (2015). [PubMed: 26555489]
26. Ertugrul IO, Jeni LA, Ding W. & Cohn JF AFAR: A Deep Learning Based Tool for Automated Facial Affect Recognition. Proc. Int. Conf. Autom. Face Gesture Recognit. 2019, (2019).
27. Gibson WS et al. The Impact of Mirth-Inducing Ventral Striatal Deep Brain Stimulation on Functional and Effective Connectivity. Cereb. Cortex 27, 2183–2194 (2017). [PubMed: 27001680]
28. Provenza Nicole R., Gelin Luiz Fernando Fracassi, Mahaphanit Wasita, McGrath Mary C., Dastin-van Rijn Evan M., Fan Yunshu, Dhar Rashi, Frank Michael J., Restrepo Maria I., Goodman Wayne K., Borton David A.. Honeycomb: a template for reproducible psychophysiological tasks for clinic, laboratory, and home use. Brazilian Journal of Psychiatry in press, (2021).
29. Mataix-Cols D. et al. Symptom stability in adult obsessive-compulsive disorder: data from a naturalistic two-year follow-up study. Am. J. Psychiatry 159, 263–268 (2002). [PubMed: 11823269]
30. Nota JA, Gibb BE & Coles ME Obsessions and Time of Day: A Self-Monitoring Study in Individuals With Obsessive-Compulsive Disorder. J. Cogn. Psychother. 28, 134–144 (2014). [PubMed: 32759112]
31. Gerald JH & George SH Self-report: Psychology's four-letter word. Am. J. Psychol. 123, 181–188 (2010). [PubMed: 20518434]
32. Powers R. et al. Smartwatch inertial sensors continuously monitor real-world motor fluctuations in Parkinson's disease. Science Translational Medicine vol. 13 eabd7865 (2021).
33. Cuthbert BN & Insel TR Toward the future of psychiatric diagnosis: the seven pillars of RDoC. BMC Med. 11, 126 (2013). [PubMed: 23672542]
34. Gillan CM, Kosinski M, Whelan R, Phelps EA & Daw ND Characterizing a psychiatric symptom dimension related to deficits in goal-directed control. Elife 5, (2016).
35. Provenza NR et al. Decoding task engagement from distributed network electrophysiology in humans. J. Neural Eng. 16, 056015 (2019). [PubMed: 31419211]
36. Widge AS et al. Deep brain stimulation of the internal capsule enhances human cognitive control and prefrontal cortex function. Nat. Commun. 10, 1536 (2019). [PubMed: 30948727]

37. Basu I. et al. Closed loop enhancement and neural decoding of human cognitive control. Cold Spring Harbor Laboratory 2020.04.24.059964 (2020) doi:10.1101/2020.04.24.059964.
38. Smith EH et al. Widespread temporal coding of cognitive control in the human prefrontal cortex. Nat. Neurosci. 22, 1883–1891 (2019). [PubMed: 31570859]
39. Ung H. et al. Intracranial EEG fluctuates over months after implanting electrodes in human brain. J. Neural Eng. 14, 056011 (2017). [PubMed: 28862995]
40. Grover S, Nguyen JA, Viswanathan V. & Reinhart RMG High-frequency neuromodulation improves obsessive–compulsive behavior. Nat. Med. 27, 232–238 (2021). [PubMed: 33462447]
41. Scangos KW, Makhoul GS, Sugrue LP, Chang EF & Krystal AD State-dependent responses to intracranial brain stimulation in a patient with depression. Nat. Med. (2021) doi:10.1038/s41591-020-01175-8.
42. Figee M. & Mayberg H. The future of personalized brain stimulation. Nat. Med. (2021) doi:10.1038/s41591-021-01243-7.
43. Mercier MR et al. Evaluation of cortical local field potential diffusion in stereotactic electroencephalography recordings: A glimpse on white matter signal. Neuroimage 147, 219–232 (2017). [PubMed: 27554533]
44. Haber SN, Yendiki A. & Jbabdi S. Four Deep Brain Stimulation Targets for Obsessive-Compulsive Disorder: Are They Different? Biol. Psychiatry (2020) doi:10.1016/j.biopsych.2020.06.031.
45. Li N. et al. Toward a unified connectomic target for deep brain stimulation in obsessive-compulsive disorder. doi:10.1101/608786.
46. Figee M. et al. Deep brain stimulation restores frontostriatal network activity in obsessive-compulsive disorder. Nature Neuroscience vol. 16 386–387 (2013). [PubMed: 23434914]
47. Olsen ST et al. Case Report of Dual-Site Neurostimulation and Chronic Recording of Cortico-Striatal Circuitry in a Patient With Treatment Refractory Obsessive Compulsive Disorder. Front. Hum. Neurosci. 14, 423 (2020).
48. Wu H. et al. Closing the loop on impulsivity via nucleus accumbens delta-band activity in mice and man. Proc. Natl. Acad. Sci. U. S. A. 115, 192–197 (2018). [PubMed: 29255043]
49. Sildatke E. et al. Error-Related Activity in Striatal Local Field Potentials and Medial Frontal Cortex: Evidence From Patients With Severe Opioid Abuse Disorder. Front. Hum. Neurosci. 14, 627564 (2020). [PubMed: 33597851]
50. Lega BC, Kahana MJ, Jaggi J, Baltuch GH & Zaghloul K. Neuronal and oscillatory activity during reward processing in the human ventral striatum. Neuroreport 22, 795–800 (2011). [PubMed: 21975313]
51. Neumann W-J et al. Different patterns of local field potentials from limbic DBS targets in patients with major depressive and obsessive compulsive disorder. Mol. Psychiatry 19, 1186–1192 (2014). [PubMed: 24514569]
52. Miller KJ, Prieto T, Williams NR & Halpern CH Case Studies in Neuroscience: The electrophysiology of a human obsession in nucleus accumbens. J. Neurophysiol. 121, 2336–2340 (2019). [PubMed: 31017846]
53. Schwabe K. et al. Oscillatory activity in the BNST/ALIC and the frontal cortex in OCD: acute effects of DBS. J. Neural Transm. (2021) doi:10.1007/s00702-020-02297-6.
54. Frank AC et al. Identification of a personalized intracranial biomarker of depression and response to DBS therapy. Brain Stimulation vol. 14 1002–1004 (2021). [PubMed: 34175247]
55. Tyagi H. et al. A Randomized Trial Directly Comparing Ventral Capsule and Anteromedial Subthalamic Nucleus Stimulation in Obsessive-Compulsive Disorder: Clinical and Imaging Evidence for Dissociable Effects. Biol. Psychiatry 85, 726–734 (2019). [PubMed: 30853111]
56. Liebrand LC et al. Individual white matter bundle trajectories are associated with deep brain stimulation response in obsessive-compulsive disorder. Brain Stimul. 12, 353–360 (2019). [PubMed: 30522916]
57. Figee M. et al. Dysfunctional reward circuitry in obsessive-compulsive disorder. Biol. Psychiatry 69, 867–874 (2011). [PubMed: 21272861]
58. Eijsker N, van Wingen G, Smolders R, Smit DJA & Denys D. Exploring the Role of the Nucleus Accumbens in Adaptive Behavior Using Concurrent Intracranial and Extracranial Electrophysiological Recordings in Humans. eNeuro 7, (2020).

59. Stenner M-P et al. Cortical drive of low-frequency oscillations in the human nucleus accumbens during action selection. Journal of Neurophysiology vol. 114 29–39 (2015). [PubMed: 25878159]
60. Smith EE et al. A brief demonstration of frontostriatal connectivity in OCD patients with intracranial electrodes. Neuroimage 220, 117138 (2020). [PubMed: 32634597]
61. Storch EA et al. Psychometric analysis of the Yale-Brown Obsessive–Compulsive Scale Second Edition Symptom Checklist. Journal of Anxiety Disorders vol. 24 650–656 (2010). [PubMed: 20471199]
62. Goodman WK et al. The Yale-Brown Obsessive Compulsive Scale. I. Development, use, and reliability. Arch. Gen. Psychiatry 46, 1006–1011 (1989). [PubMed: 2684084]
63. Goodman WK et al. The Yale-Brown Obsessive Compulsive Scale. II. Validity. Arch. Gen. Psychiatry 46, 1012–1016 (1989). [PubMed: 2510699]
64. Fischl B. FreeSurfer. NeuroImage vol. 62 774–781 (2012). [PubMed: 22248573]
65. Jenkinson M. & Smith S. A global optimisation method for robust affine registration of brain images. Med. Image Anal. 5, 143–156 (2001). [PubMed: 11516708]
66. Jenkinson M, Bannister P, Brady M. & Smith S. Improved optimization for the robust and accurate linear registration and motion correction of brain images. Neuroimage 17, 825–841 (2002). [PubMed: 12377157]
67. Joshi A. et al. Unified framework for development, deployment and robust testing of neuroimaging algorithms. Neuroinformatics 9, 69–84 (2011). [PubMed: 21249532]
68. Felsenstein O. & Peled N. MMVT-Multi-Modality Visualization Tool. GitHub Repository. Available online at: https://github.com/pelednoam/mmvt (accessed June 1, 2020) (2017).
69. Felsenstein O. et al. Multi-Modal Neuroimaging Analysis and Visualization Tool (MMVT). arXiv [q-bio.NC] (2019).
70. Bush G, Shin LM, Holmes J, Rosen BR & Vogt BA The Multi-Source Interference Task: validation study with fMRI in individual subjects. Mol. Psychiatry 8, 60–70 (2003). [PubMed: 12556909]
71. Bush G. & Shin LM The Multi-Source Interference Task: an fMRI task that reliably activates the cingulo-frontal-parietal cognitive/attention network. Nat. Protoc. 1, 308–313 (2006). [PubMed: 17406250]
72. Voon V. et al. Decisional impulsivity and the associative-limbic subthalamic nucleus in obsessive-compulsive disorder: stimulation and connectivity. Brain 140, 442–456 (2017). [PubMed: 28040671]
73. Sellers KK et al. Analysis-rcs-data: Open-source toolbox for the ingestion, time-alignment, and visualization of sense and stimulation data from the Medtronic Summit RC+S system. Front. Hum. Neurosci. 15, (2021).
74. Ertugrul IÖ, Jeni LA & Cohn JF PAttNet: Patch-attentive deep network for action unit detection. in BMVC 114 (2019).
75. Niinuma K, Jeni LA, Ertugrul IO & Cohn JF Unmasking the devil in the details: What works for deep facial action coding? BMVC 2019, (2019).
76. Yang L. et al. FACS3D-Net: 3D Convolution based Spatiotemporal Representation for Action Unit Detection. in 2019 8th International Conference on Affective Computing and Intelligent Interaction (ACII) 538–544 (2019). doi:10.1109/ACII.2019.8925514.
77. Jeni LA, Cohn JF & Kanade T. Dense 3D Face Alignment from 2D Video for Real-Time Use. Image Vis. Comput. 58, 13–24 (2017). [PubMed: 29731533]
78. Jeni LA & Cohn JF Person-independent 3d gaze estimation using face frontalization. in Proceedings of the IEEE conference on computer vision and pattern recognition workshops 87–95 (2016).
79. EKMAN P. Facial Action Coding System (FACS). A Human Face (2002).
80. Ekman P. & Rosenberg EL What the Face Reveals: Basic and Applied Studies of Spontaneous Expression Using the Facial Action Coding System (FACS). (Oxford University Press, 2005).
81. Zhang Z. et al. Multimodal spontaneous emotion corpus for human behavior analysis. in Proceedings of the IEEE Conference on Computer Vision and Pattern Recognition 3438–3446 (2016).

82. Cowen AS et al. Sixteen facial expressions occur in similar contexts worldwide. Nature 589, 251–257 (2021). [PubMed: 33328631]
83. Baker J, Haltigan JD & Messinger DS Non-Expert Ratings of Infant and Parent Emotion: Concordance with Expert Coding and Relevance to Early Autism Risk. Int. J. Behav. Dev. 34, 88–95 (2010). [PubMed: 20436947]
84. Messinger DS, Mahoor MH, Chow S-M & Cohn JF Automated Measurement of Facial Expression in Infant–Mother Interaction: A Pilot Study. Infancy 14, 285–305 (2009). [PubMed: 19885384]
85. Prkachin KM & Solomon PE The structure, reliability and validity of pain expression: evidence from patients with shoulder pain. Pain 139, 267–274 (2008). [PubMed: 18502049]
86. Haines N, Southward MW, Cheavens JS, Beauchaine T. & Ahn W-Y Using Computer-vision and Machine Learning to Automate Facial Coding of Positive and Negative Affect Intensity. doi:10.1101/458380.
87. Hammal Z, Cohn JF & George DT Interpersonal Coordination of HeadMotion in Distressed Couples. IEEE Transactions on Affective Computing 5, 155–167 (2014). [PubMed: 26167256]
88. Hammal Z, Cohn JF, Heike C. & Speltz ML Automatic measurement of head and facial movement for analysis and detection of infants' positive and negative affect. Front. ICT 2, (2015).
89. Hammal Z, Cohn JF & Messinger DS Head Movement Dynamics During Play and Perturbed Mother-Infant Interaction. IEEE Trans Affect Comput 6, 361–370 (2015). [PubMed: 26640622]
90. Hammal Z. et al. Dynamics of Face and Head Movement in Infants with and without Craniofacial Microsomia: An Automatic Approach. Plast Reconstr Surg Glob Open 7, e2081 (2019). [PubMed: 30859039]
91. Dibeklioğlu H, Hammal Z. & Cohn JF Dynamic Multimodal Measurement of Depression Severity Using Deep Autoencoding. IEEE Journal of Biomedical and Health Informatics 22, 525–536 (2018). [PubMed: 28278485]
92. Kacem A, Hammal Z, Daoudi M. & Cohn J. Detecting Depression Severity by Interpretable Representations of Motion Dynamics. Proc. Int. Conf. Autom. Face Gesture Recognit. 2018, 739–745 (2018). [PubMed: 30271308]
93. Cohn JF et al. Automated Affect Detection in Deep Brain Stimulation for Obsessive-Compulsive Disorder: A Pilot Study. Proc ACM Int Conf Multimodal Interact 2018, 40–44 (2018). [PubMed: 30511050]
94. Ding Y. et al. Automated Detection of Optimal DBS Device Settings. in Companion Publication of the 2020 International Conference on Multimodal Interaction 354–356 (Association for Computing Machinery, 2020). doi:10.1145/3395035.3425354.

Figure 1: Streaming of intracranial electrophysiology data in the clinic and at home.

(Top left) Data collection in the clinic during DBS programming. Streaming intracranial electrophysiology (Local Field Potentials, LFP) from the Summit RC+S®, along with EEG, EKG, BVP, and video. (Top right) Data collection at home during symptom provocation (e.g., compulsive hand washing). Streaming LFP and capturing self-reported intensity of OCD symptoms on phone. (Bottom) Data collection at home during sleep. Streaming LFP and capturing self-reported start and stop time of sleep on iPhone.

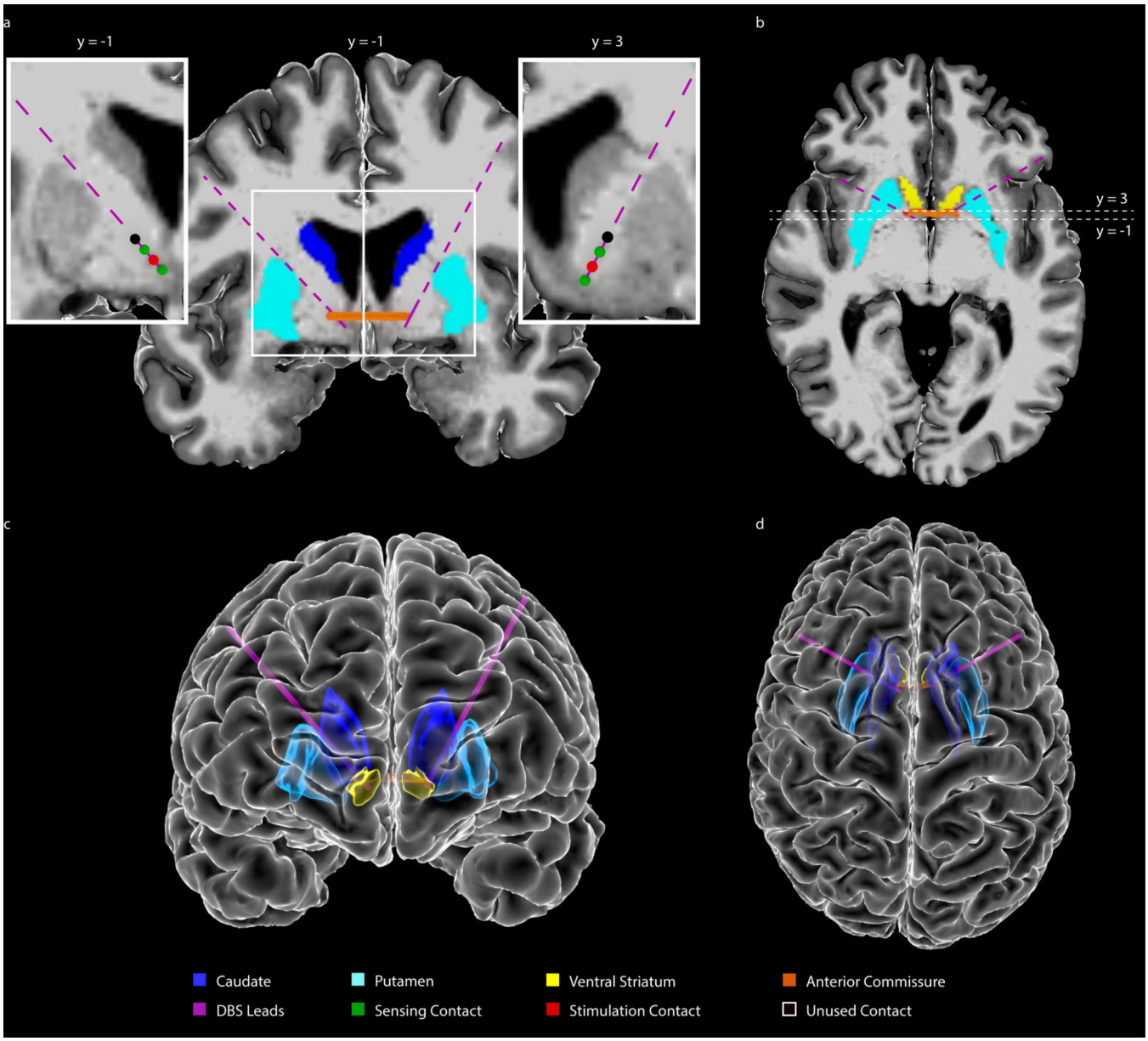

Figure 2: Anatomical localization of DBS lead placement.

(A,B) Coronal (A) and axial (B) T1-weighted (T1w) MRI in radiographic convention from participant P4 overlaid with reconstructed DBS lead trajectories. Colored regions indicate anterior commissure (AC), caudate, putamen, and ventral striatum (VS). The MRI slice shown is immediately posterior (A; coronal) or inferior (B; axial) to the most ventral contact. Enlarged coronal slices (corresponding to white box outlines in panel A) showing DBS contact locations in each hemisphere are shown on either side of the full coronal slice. Green spheres indicate sensing contacts, red spheres indicate stimulating contacts, black spheres indicate contacts that were used for neither stimulation nor sensing. Here the tip of the left lead was targeted to the VS and the tip of the right lead was targeted to the bed nucleus of the stria terminalis (BNST). Enlarged slices shown are immediately posterior to the most ventral contact in each hemisphere. Anterior-posterior slice location (*y*)

is referenced to the posterior border of the AC, which is defined as *y*=0. (D,E) Front (D) and top-down (E) view of the reconstructed cortical surface, subcortical structures, DBS leads, and AC, shown in radiographic convention.

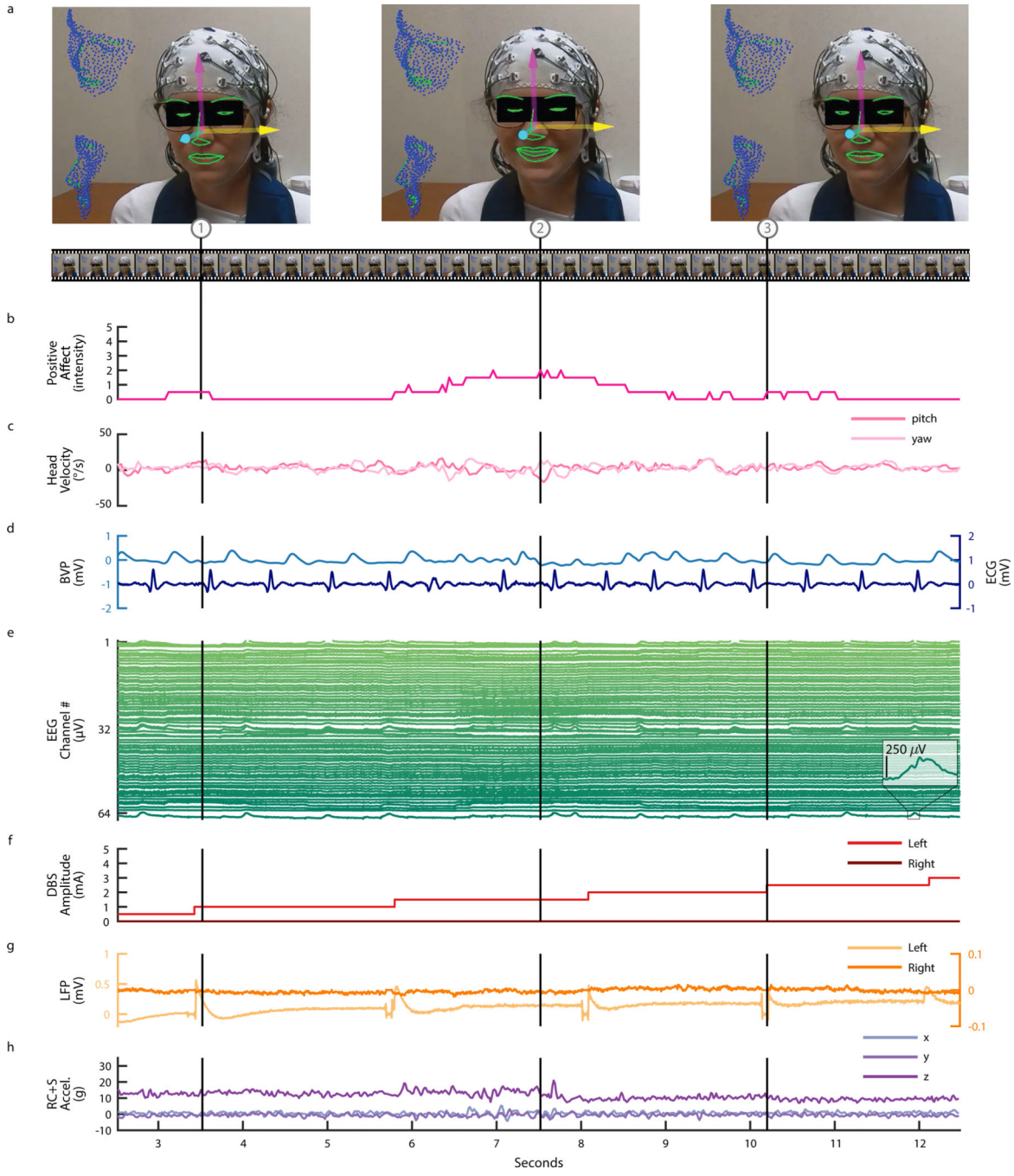

Figure 3: Intracranial VS LFP synchronized with continuous affect estimation during DBS programming for OCD.

Data shown corresponds to the initial DBS programming session for participant P5. (A) Video of the face (used with permission) was used to do automatic 3D face tracking. Arrows indicate the tracked three degrees of freedom of head pose. The contours of tracked key facial parts are highlighted in green. The three video frames (1, 2, and 3) shown correspond to the timepoints indicated by the vertical lines. (B) Estimation of positive affect on a scale of zero to five based on facial action units 6 and 12. (C) Estimation of head velocity in terms of yaw and pitch in units of degrees of displacement per second. (D) Blood volume pulse

(BVP) and electrocardiogram (ECG). (E) 64 channel EEG. (F) DBS amplitude. (G) Bilateral (left and right hemisphere) ventral striatum LFP recordings. (H) RC+S® acceleration (xyz).

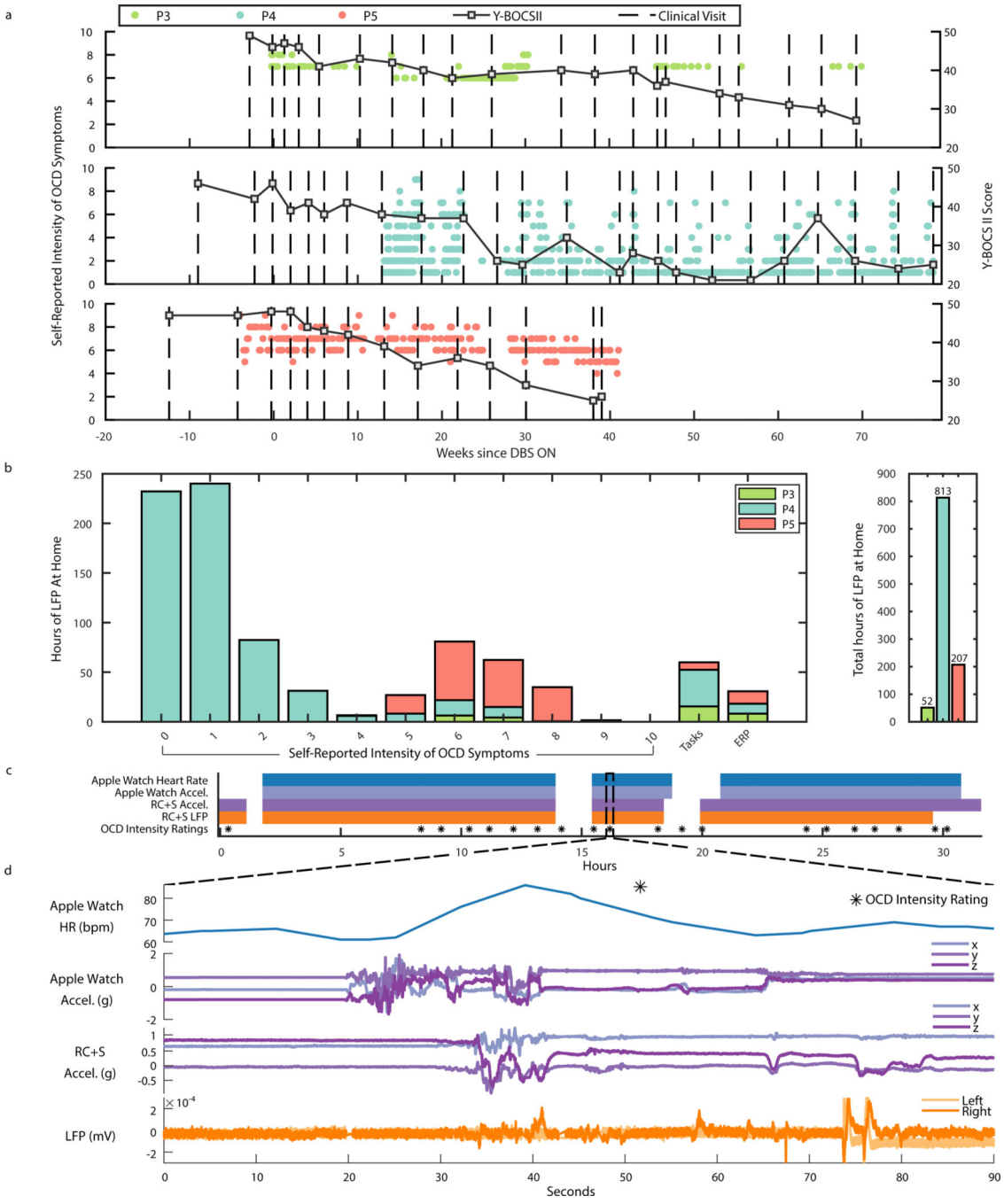

Figure 4: At home symptom monitoring synchronized with ecologically valid intracranial electrophysiology.

(A) Y-BOCS II scores, and self-reported intensity of OCD symptoms over weeks since DBS ON in P3, P4, and P5. Square black scatter points indicate Y-BOCS II scores. Circular scatter points indicate one symptom intensity rating from 0–10, and vertical dotted lines denote DBS programming clinical visits. (B) Number of hours of LFP data collected at home for P3, P4, and P5 corresponding to self-reported intensity of OCD symptoms ratings, behavioral tasks, ERP sessions, and in total. (C) Example data availability plot for at-home sprint recording over 32 hours, completed by participant P4. Shaded portions indicate data

availability for Apple watch heart rate, Apple watch acceleration, RC+S® acceleration, RC+S® LFP, and OCD intensity ratings. (D) 90 seconds of example data corresponding to dotted line callout in panel C.

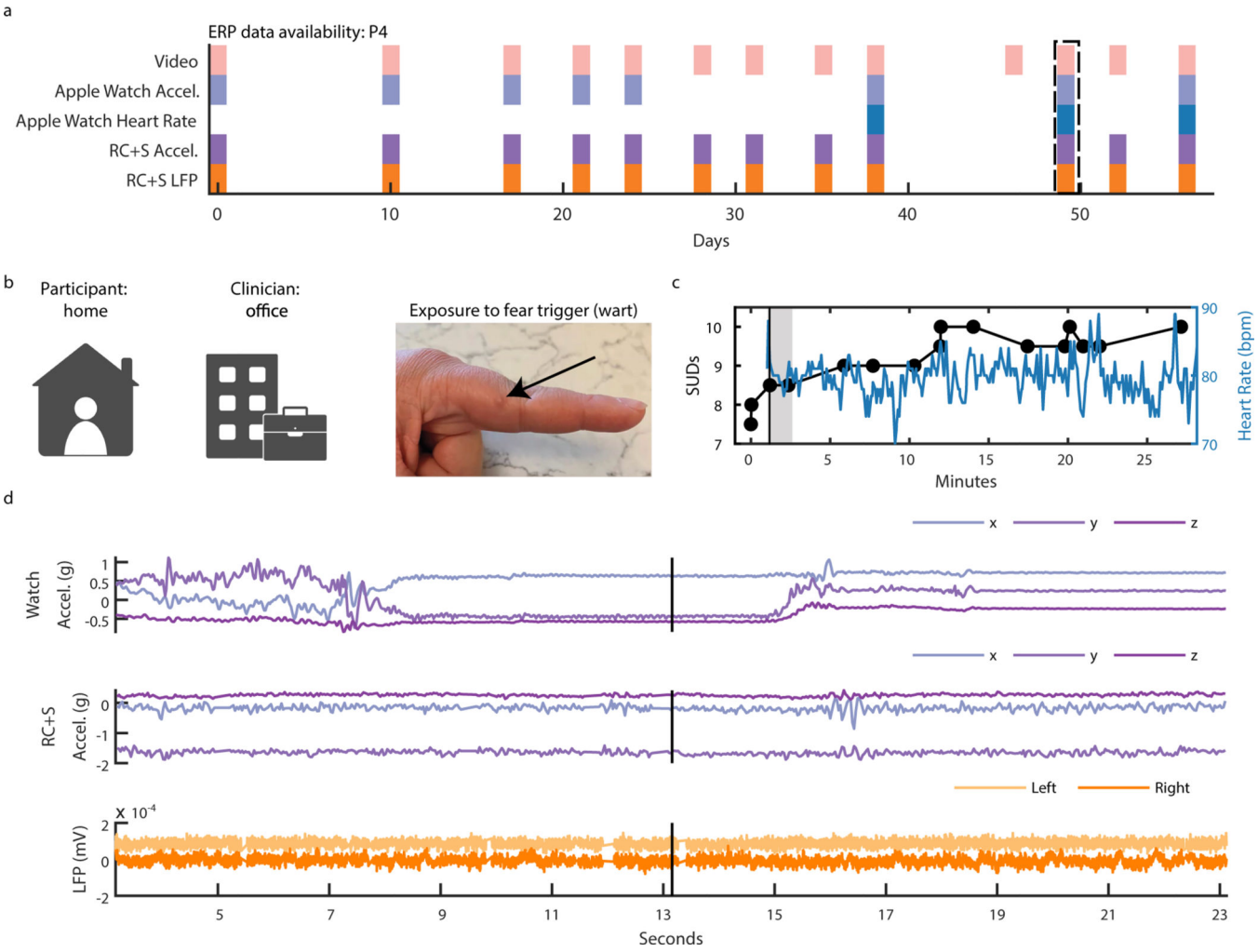

Figure 5: Intracranial electrophysiology during Exposure and Response Prevention Teletherapy at home with Participant P4.

(A) Calendar availability plot of ERP sessions for participant P4, over days since the first ERP session. Shaded portions indicate data availability for ERP video, Apple watch heart rate, Apple watch acceleration, RC+S® acceleration, and RC+S® LFP. Rectangular dotted line corresponds to the ERP session example data shown in panels B-D. (B) Video of participant P4 (left), clinician (center), and image of exposure (right). (C) Time-course in minutes of self-reported Subjective Units of Distress (SUDs) ratings and heart rate collected via the Apple Watch throughout the ERP session. Vertical black line denotes the start of the exposure period. Gray shaded area corresponds to the time period shown in supplemental video 2. (D) 20 seconds of example data synchronized to video, including apple watch acceleration, RC+S® acceleration, and two bipolar LFP channels. Vertical black line corresponds to the video frame shown in panel B.

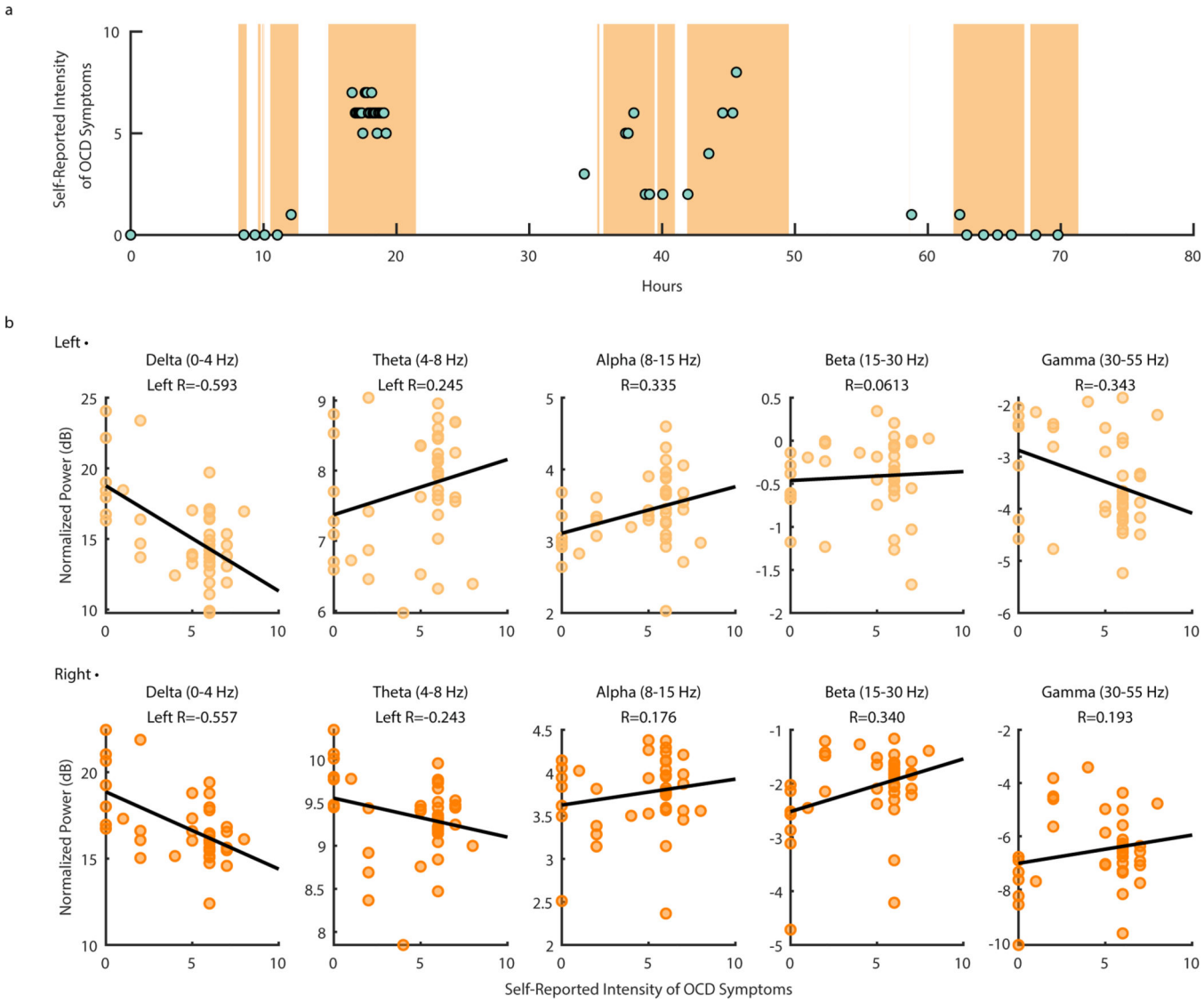

Figure 6: Ventral Capsule/Ventral Striatum spectral power shows correlations with OCD symptom intensity during P4 natural exposures at home.

(A) Self-reported intensity of OCD symptoms (scatter points) shown over time in hours with LFP data availability (orange shading). (B) Normalized left (top row) and right (bottom row) VC/VS spectral power in Delta (0–4 Hz), Theta (4–8 Hz), Alpha (8–15 Hz), Beta (15–30 Hz), and Gamma (30–55 Hz) (from left to right) vs. self-reported OCD symptom intensity from zero to 10. Black lines represent the line of least squares. R values correspond to the coefficient of correlation.